

MICROCOPY RESOLUTION TEST CHART

NATIONAL BUREAU OF STANDARDS-1963-A

AFWAL-TR-80-2013

LEVEL

2
e⁵

ADA 083245

THREE-DIMENSIONAL FINITE-ELEMENT ELASTIC ANALYSIS
OF A THERMALLY CYCLED DOUBLE-EDGE WEDGE GEOMETRY
SPECIMEN

Sandra K. Drake, Richard J. Hill, Jeffrey L. Kladden
Propulsion Branch
Turbine Engine Division

Peter T. Bizon, Bruce P. Guilliams
Lewis Research Center

March 1980

TECHNICAL REPORT AFWAL-TR-80-2013

Final Report for Period 1 June 1977 to 1 January 1979

Approved for public release; distribution unlimited.

DDC FILE COPY.

AERO PROPULSION LABORATORY
AIR FORCE WRIGHT AERONAUTICAL LABORATORIES
AIR FORCE SYSTEMS COMMAND
WRIGHT-PATTERSON AIR FORCE BASE, OHIO 45433

DTIC
ELECTE
APR 22 1980
S D
E

80 4 21 129

NOTICE

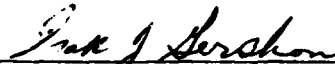
When Government drawings, specifications, or other data are used for any purpose other than in connection with a definitely related Government procurement operation, the United States Government thereby incurs no responsibility nor any obligation whatsoever; and the fact that the government may have formulated, furnished, or in any way supplied the said drawings, specifications, or other data, is not to be regarded by implication or otherwise as in any manner licensing the holder or any other person or corporation, or conveying any rights or permission to manufacture, use, or sell any patented invention that may in any way be related thereto.

This report has been reviewed by the Information Office (OI) and is releasable to the National Technical Information Service (NTIS). At NTIS, it will be available to the general public, including foreign nations.

This technical report has been reviewed and is approved for publication.



Project Engineer
Propulsion Mechanical Design
Propulsion Branch
Turbine Engine Division



Technical Area Manager
Propulsion Mechanical Design
Propulsion Branch
Turbine Engine Division

FOR THE COMMANDER



H. I. Bush
Deputy Director
Turbine Engine Division

"If your address has changed, if you wish to be removed from our mailing list, or if the addressee is no longer employed by your organization please notify AFWAL/POTP, W-PAFB, OH 45433 to help us maintain a current mailing list".

Copies of this report should not be returned unless return is required by security considerations, contractual obligations, or notice on a specific document.

SECURITY CLASSIFICATION OF THIS PAGE (When Data Entered)

REPORT DOCUMENTATION PAGE		READ INSTRUCTIONS BEFORE COMPLETING FORM
1. REPORT NUMBER 14 AFWAL-TR-80-2013	2. GOVT ACCESSION NO.	3. RECIPIENT'S CATALOG NUMBER
4. TITLE (and Subtitle) 6 THREE DIMENSIONAL FINITE-ELEMENT ANALYSIS OF A THERMALLY CYCLED DOUBLE-EDGE WEDGE GEOMETRY SPECIMEN	Elastic	5. TYPE OF REPORT & PERIOD COVERED Final Report 6/1/77 to 1/1/79
		6. PERFORMING ORG. REPORT NUMBER
7. AUTHOR(S) 11 Sandra K. Drake* Jeffrey L. Kladden* Richard J. Hill* Bruce P. Williams** Peter T. Bizon**		8. CONTRACT OR GRANT NUMBER(S) 12661
9. PERFORMING ORGANIZATION NAME AND ADDRESS Aero Propulsion Laboratory (POTP) Air Force Wright Aeronautical Laboratories Wright-Patterson AFB, Ohio 45433		10. PROGRAM ELEMENT, PROJECT, TASK AREA & WORK UNIT NUMBERS Program Element 62203F Project 3066, Task 3066 2.1 Work Unit 30661252
11. CONTROLLING OFFICE NAME AND ADDRESS Aero Propulsion Laboratory (POTP) Air Force Wright Aeronautical Laboratories Wright-Patterson AFB, Ohio 45433	11	12. REPORT DATE March 1980
		13. NUMBER OF PAGES 49
14. MONITORING AGENCY NAME & ADDRESS (if different from Controlling Office)		15. SECURITY CLASS. (of this report) Unclassified 12661
15a. DECLASSIFICATION DOWNGRADING SCHEDULE		
16. DISTRIBUTION STATEMENT (of this Report) Approved for public release, distribution unlimited.		
17. DISTRIBUTION STATEMENT (of the abstract entered in Block 20, if different from Report)		
18. SUPPLEMENTARY NOTES *Aero Propulsion Laboratory **Lewis Research Center		
19. KEY WORDS (Continue on reverse side if necessary and identify by block number) Thermal Analysis Three Dimensional Finite Element Analysis Blade Analysis Stress Analysis of Prismatic Bar		
20. ABSTRACT (Continue on reverse side if necessary and identify by block number) An elastic stress analysis was performed on a wedge specimen (prismatic bar with double-edge wedge cross-section) subjected to thermal cycles in fluidized beds. Five alloys (IN 100, Mar-M 200, Mar-M 302, NASA TAZ-8A, and Rene 80) subjected to the same thermal cycling condition were analyzed. This condition was alternate 3 minute immersions in fluidized beds maintained at 316° and 1088°C (600° and 1990°F). The analyses were performed as a joint effort of two laboratories using different models and computer programs (NASTRAN and IS03DQ). Stress, strain, and temperature results are presented.		

DD FORM 1 JAN 73 1473 EDITION OF 1 NOV 65 IS OBSOLETE

SECURITY CLASSIFICATION OF THIS PAGE (When Data Entered)

3926

PREFACE

This report covers work carried out as a joint program between engineers from the Aero Propulsion Laboratory (AFWAL/POTP) and the National Aeronautics and Space Administration (NASA) Lewis Research Center under in-house project 30661252. The objective of this effort was to analytically determine the elastic stress/strain-temperature-time history at the critical location for a double edge wedge geometry specimen cycled in fluidized beds.

The research was conducted from June 1977 to January 1979.

PRECEDING PAGE BLANK-NOT FILMED

Accession For	
NTIS GRA&I	<input checked="" type="checkbox"/>
DDC TAB	<input type="checkbox"/>
Unannounced	<input type="checkbox"/>
Justification	
By _____	
Distribution/_____	
Distribution Codes	
Dist	Mail and/or special
A	

TABLE OF CONTENTS

SECTION		PAGE
I	INTRODUCTION	1
II	INPUT FOR COMPUTER PROGRAMS	3
	1. Wedge Geometry	3
	2. Alloy Properties	3
	3. Temperature Loading	4
III	DESCRIPTION OF ANALYSES	5
	1. IS03DQ Computer Program	5
	2. NASTRAN Computer Program	7
IV	RESULTS AND DISCUSSION	8
	1. Comparison of IS03DQ and NASTRAN Analysis	8
	2. Critical Locations	9
	3. Minimum and Maximum Longitudinal Strain	10
V	SUMMARY OF RESULTS AND CONCLUSIONS	12
	REFERENCES	42

PRECEDING PAGE BLANK-NOT FILMED

LIST OF ILLUSTRATIONS

FIGURE		PAGE
1	Double-edge Wedge. (All dimensions in cm (in.) unless indicated otherwise.)	16
2	Schematic of Fluidized Bed Test Facility	19
3	Temperature of Mid-chord at Mid-span at Various Times after Immersion into the Fluidized Beds	20
4	Comparisons Determined by Using ISO3DQ and NASTRAN Computer Programs (Using the Models in Figure 1) for IN 100 Alloy After 15 Seconds Heating in the 1088°C (1990°F) Fluidized Bed	25
5	Temperature, Longitudinal Strain, and Longitudinal Stress at Critical Locations During a Typical Fluidized Bed Cycle	27
6	Temperature, Stress, and Strain Distribution of Mid-chord at Time of Minimum Leading Edge Longitudinal Strain. ($F = 9/5 C + 32$)(1 ksi = 6.89×10^6 N/m ²).	32
7	Temperature, Stress, and Strain Distribution of Mid-chord at Time of Maximum Leading Edge Longitudinal Strain. ($F = 9/5 C + 32$)(1 ksi = 6.89×10^6 N/m ²).	37

SECTION I

INTRODUCTION

One important area of research necessary for advancing the technology of aircraft gas turbine engines is the accurate assessment of the life prediction procedures used for hot section blades and vanes. In order to further develop and evaluate life prediction methods, this program tested in the laboratory simulated hardware components using carefully controlled conditions. Comparison of the experimentally measured life to that which is analytically predicted is used as a means of evaluating life prediction theories.

The experimental laboratory method used in this program for measuring thermal fatigue life is the cycling of wedge (blade-like) specimens in fluidized beds. Such tests have been shown to provide life and transient temperature data under carefully controlled conditions. Reference 1 contains a compilation of such data including a description of the facility and test procedure. References 2 - 9 contain incremental portions of such data relative to the evaluations described in this paper.

The objective of this investigation was to analytically determine the elastic stress/strain-temperature-time history at the critical location for a double-edge wedge geometry specimen cycled in fluidized beds. This was performed as a joint program between the engineers from the Air Force and the National Aeronautics and Space Administration (NASA) and utilized conventional three-dimensional finite element elastic analysis techniques. Engineers at the Aero Propulsion Laboratory (AFWAL/POTP) used the IS03DQ computer program while the NASA/Lewis Research Center engineers used the NASTRAN program. The alloys were IN 100, Mar-M 200, Mar-M 302, NASA TAZ-8A, and Rene 80.

Two fluidized beds were used for rapidly heating and cooling the specimens. The specimens were in the form of prismatic bars with a double-wedge constant cross-sectional geometry. These specimens failed by thermal fatigue cracking which is usually the predominant failure mode of aircraft engine first stage turbine blades and vanes. Thermal fatigue is defined as the cracking of a material induced from cyclic

stresses and strains caused by repeated temperature changes. The cycling condition was alternate 3 minute immersions in fluidized beds maintained at 316° and 1088°C (600° and 1990°F). The cycling test condition chosen was one which resulted in thermal fatigue cracking in a reasonable number of cycles.

Due to symmetry, a discretized model of only a quarter of the double-edge wedge geometry was necessary for analysis. First, a model with a fine mesh for IN 100 alloy for a severe time increment (15 seconds after immersion in the heating bed) was analyzed using the NASTRAN computer program. Then, a model with various coarse meshes for the same conditions was analyzed using the ISO3DQ program. A coarse mesh model for the ISO3DQ analysis was selected which gave essentially the same results as using the fine mesh model with the NASTRAN analysis. The remaining combinations were then analyzed using the coarse mesh model and the ISO3DQ program. Such analyses provide the strain range and stress/strain-temperature-time history so important for evaluation of life prediction theories. The turbine component life prediction methods currently being studied at NASA/Lewis are discussed in References 10 - 15. Results of similar analyses for a single-edge wedge geometry specimen are given in Reference 16.

SECTION II
INPUT FOR COMPUTER PROGRAMS

The alloys and test condition for the five alloys are given in Table 1. The necessary inputs to perform the analyses were: (1) the geometry of the double-edge wedge, (2) the elastic and physical material properties of the five alloys, and (3) a complete temperature distribution at various times throughout the cycle. This section gives a detailed description of these inputs.

1. WEDGE GEOMETRY

The geometry for the double-edge wedge is shown in Figure 1(a). The computer plots of the models used for analysis and a typical element are shown in Figure 1(b) for the ISO3DQ program and in Figure 1(c) for the NASTRAN program. The model for both programs "squared-off" the leading edge radius to a 1.02 mm (0.040 in.) length and the trailing edge radius to a 1.53 mm (0.060 in.) length. Otherwise the models duplicated the geometry of the wedge exactly. Detailed discussion of the modeling is given in Section III Description of Analyses.

2. ALLOY PROPERTIES

The temperature independent and temperature dependent alloy properties used for the elastic analyses are given in Tables 2 and 3, respectively. The properties required for the analyses were Poisson's ratio, modulus of elasticity, and the mean coefficient of thermal expansion. The programs required a value for density to obtain results (zero mass elements were not permitted) although the results are independent of density. The properties for all alloys except the mean coefficient of thermal expansion for NASA TAZ-8A alloy were obtained from References 17 and 18. The mean coefficient of thermal expansion for NASA TAZ-8A was independently determined. This and all data in Reference 17 were determined from the same heat used for fabricating the double-edge wedge test and calibration specimens.

3. TEMPERATURE LOADING

The transient temperature loading on the double-edge wedges was determined from thermocouple data. Calibration specimens of the five alloys were instrumented chordwise at the mid-span with five embedded thermocouples and cycled in the fluidized beds (schematically shown in Figure 2). The location of the thermocouples at the wedge cross-section is shown in Figure 3. The Inconel 600 sheathed thermocouples were mounted in grooves milled in the surface of the specimen and secured by a ceramic cement. The grooves were 0.56 mm (0.022 in.) wide and 0.5 mm (0.02 in.) deep. Other details of the installation and procedure are given in Reference 1. The thermocouple outputs were cross-plotted to give temperatures of the mid-chord at the mid-span at various time increments after immersion into the fluidized beds. These data are presented as Figure 3 for the five cases analyzed. It was assumed that there was no temperature gradient through the thickness of the wedge.

Another set of thermocouple data was taken with five thermocouples mounted along the leading edge over half the span. These data revealed a longitudinal (along the span of the wedge) temperature gradient which varied with the different time increments. The maximum variation was about 16 percent greater at the ends of the wedge compared to the mid-span and occurred after 30 seconds of heating. However, for any one time increment it was found that the ratio of the leading edge mid-span temperature to that of any other span location was nominally the same for the five investigated cases. A least square's best fit parabola was determined for each time increment and this is presented in Table 4. This parabolic temperature variation along the span was assumed over the complete chord of the wedge.

The temperatures at mid-span were determined from the appropriate plot in Figure 3. For locations other than mid-span, the temperatures were determined by using the mid-span temperature modified by the values given in Table 4. Therefore, the use of Figure 3 and Table 4 determined the temperature distribution at any point of the wedge.

SECTION III DESCRIPTION OF ANALYSIS

Both computer programs used three-dimensional finite-element procedures to obtain an elastic analysis of the double-edge wedge geometry specimen. The NASTRAN program was used to obtain an analysis only for IN 100 alloy for the time increment 15 seconds after immersion into the heating bed. The IS03DQ analysis was performed for the 17 heating and 17 cooling time increments (distributed over the 3 minute immersion time) for each of the five alloys as shown in Figure 3.

The IS03DQ program was developed under contract by the Air Force for elastic analysis - specifically aircraft gas turbine blades, vanes, and disks. The NASTRAN program was developed by NASA for elastic analysis of generalized structures. Documentation of the IS03DQ program includes a descriptive report (Reference 19) and a user's manual (Reference 20). Documentation of the NASTRAN program includes a theoretical manual (Reference 21), a programmer's manual (Reference 22), a user's manual (Reference 23), and a demonstration problem manual (Reference 24). For general information on the programs, the reader is referred to these manuals. Specific information on how the wedge was modeled and analyzed using these programs is presented in the following sections.

1. IS03DQ COMPUTER PROGRAM

The model for the double-edge wedge was one-fourth of the structure as shown in Figure 1(b). There are reflective planes of symmetry at the mid-chord and mid-span for this structure. The nodal constraints on this model (using the axis notation given in Figure 1(b)) are:

- (1) No z-displacement for nodes on the mid-span plane because of reflective symmetry.
- (2) No y-displacement for nodes on the mid-chord plane because of reflective symmetry.
- (3) No x-displacement for the two nodes at $x=0.0$ of the mid-span plan to obtain a reference for displacements.

The coarse mesh model selected consisted of 306 nodes for the 64 isoparametric elements. A typical element is shown in Figure 1(b). The element had mid-point nodes along the x-direction but not the y- and z-directions so that each element consisted of twelve nodes. The discretization, including element and nodal identification, was done using a mesh generator. This pre-processor (MESH3) is part of the IS03DQ family of programs. This program required only the cross-section geometry of the wedge and some mesh parameters for the geometry input. The maximum aspect ratio for the elements was less than 13.

Values for the two temperature dependent properties (modulus of elasticity and mean coefficient of thermal expansion) were entered into the program as segments of Table 3. This table gives the modulus of elasticity and mean coefficient of thermal expansion for each alloy at 56°C (100°F) temperature increments. Six values of modulus and thermal expansion for six given temperature increments (Table 3) were put into the program. The program selected the value for the two temperature dependent properties for each node by using the nodal temperature to linearly interpolate within the table.

The temperature loading was entered by means of a temperature table of 13 chord temperatures at four different span locations. The program assigned a temperature to each node by weighted interpolation. Because temperatures were assigned to nodes rather than elements, a straight line gradient between adjacent nodes was assumed.

The output selected from the IS03DQ program were the displacements, strains, and stresses. All of these values were determined at the node points. This set of data was put on tape for use by another program called PROUT3. The latter program, part of the IS03DQ family, allows the amount and format of the output to be varied without requiring the complete program to be rerun. Both the MESH3 (pre-processor) and PROUT3 programs have plot capability.

The IS03DQ family of programs were run on the Wright-Patterson Air Force Base CDC 6600 computer. Plots (including Figure 1(b)) were done using a Calcomp on-line plotter.

2. NASTRAN COMPUTER PROGRAM

The model for the NASTRAN analysis was similar to that used for the ISO3DQ program. One-fourth of the double-edge wedge was used considering mid-chord and mid-span planes of symmetry as shown in Figure 1(c). The nodal constraints were identical to those used in the ISO3DQ program so that a valid comparison could be made. A fine mesh was used in the NASTRAN analysis so that it might be used as the "baseline" for comparison. The model consisted of 820 nodes for the 354 CHEXA2 (hexahedral) elements. A typical element is shown in Figure 1(c). The discretization, including element and nodal identification, was done by hand - no mesh generator was used. The geometry was entered into the computer program by listing the coordinates of each node point from the origin as shown in Figure 1(c). Elements were selected so that the maximum aspect ratio for any element was always less than two.

The complete table of temperature dependent properties (modulus of elasticity and mean coefficient of thermal expansion) for IN 100 alloy was entered with 56°C (100°F) increments as given in Table 3. The program selected the value for these properties for each element by using the element temperature to linearly interpolate within this table. Since temperatures were assigned to nodes rather than elements, the element temperature was determined by the program by averaging the eight nodal temperatures. Since NASTRAN does not have the capability to input temperatures by use of equations, all temperatures were first hand calculated (using Figure 3(a) and Table 4) and then entered for each node point.

The output selected from the NASTRAN program were the displacements, single point constraint forces, and stresses. The displacements and forces were given at the node points and the stresses were given at the element centroids. Stresses at the leading and trailing edges were obtained by extrapolation of plots through the centroids of the elements.

This program was run using level 16.0 of NASTRAN on a Univac 1110 computer. The plot given in Figure 1(c) was done on a Calcomp plotter using the NASTRAN plot subroutine.

SECTION IV

RESULTS AND DISCUSSION

The results are presented and discussed in three parts. First, comparison of the IS03DQ and NASTRAN analyses for the check case are presented. Second, results for all five cases calculated by the IS03DQ program are presented at the critical location. The critical location was taken as that point on the blade which had the maximum longitudinal strain range (algebraic difference between maximum and minimum longitudinal strain) throughout the complete heating and cooling cycle. This location was on the leading edge but not at mid-span because of the longitudinal temperature gradient. Lastly, detailed computer plots for the five cases are presented at the times of both maximum and minimum longitudinal strain.

1. COMPARISON OF IS03DQ AND NASTRAN ANALYSIS

The comparison of the analyses of the double-edge wedge using IS03DQ with the coarse mesh model (Figure 1(b)) and NASTRAN with the fine mesh model (Figure 1(c)) is given in Figure 4. The comparison shows very good agreement. Both analyses were independently performed for IN 100 alloy after 15 seconds of fluidized bed heating. This alloy and time increment were selected as being approximately the most severe combination of all those studied to accentuate any differences between analyses.

Figure 4(a) gives the normal x-, y-, and z-displacements along the leading and trailing edges. These results show that the normal displacements as determined by the two methods essentially coincide.

Figure 4(b) gives the longitudinal stress along the mid-chord at one-quarter span which was the critical location for this case. These very good comparative results show that both the leading and trailing edges are in compression. This is due to the manner of testing in that the specimens were stacked so that they were heated and cooled from both the leading and trailing edges. A force balance of this cross-section showed that equilibrium requirements were satisfied.

This comparison confirmed that the ISO3DQ program using a coarse mesh model was sufficiently accurate to obtain very good quantitative results. It also gave confidence in the use of this specialized blade and disk stress analysis program.

2. CRITICAL LOCATIONS

Results for the five analyzed cases at the two critical locations (symmetrical about mid-span) as a function of time after immersion into the fluidized beds are given in Figure 5. This figure shows the temperature, and longitudinal strain and stress as a function of cycle time which occur at both critical locations on the leading edge.

In Figure 5, the temperature is the nodal temperature at the critical locations on the leading edge as determined from the temperature loading that was input to the ISO3DQ program. The procedure used to determine this temperature is given in the section ISO3DQ Computer Program.

Both the longitudinal leading edge stress and strain show very steep gradients for about the first 10 seconds of immersion in both the heating or cooling beds. The results show that the leading edge goes into compression upon immersion into the heating bed. As the specimen reaches a steady-state condition, the stresses and strains approach zero. Upon immersion into the cooling bed, the leading edge goes into tension followed by a gradual drop-off to low stress and strain by the end of the cooling cycle.

The maximum longitudinal strain range for the cases analyzed varied from 0.53 to 0.82 percent (Figure 5). Mar-M 200 and Rene 80 demonstrated the highest strain range of about 0.8 percent. Mar-M 302 alloy showed the lowest strain range of the five alloys analyzed.

Due to symmetry, the analysis showed three critical locations on the leading edge which were 0.64 cm (0.25 in.), 1.27 cm (0.5 in.) or 2.54 cm (1.0 in.) away from mid-span for the five cases evaluated. Preliminary experimental data in fluidized bed tests for some of the cases indicate that cracks are initiated in this region.

The leading edge of the double-edge wedge is in a uniaxial state of stress. On the free surfaces, the normal x- and y-stresses (refer to Figure 1(b) for the axes convention) are zero. Therefore, the effective stress at the leading edge is equal in magnitude to the longitudinal z-stress. The x- and y-strains at the leading edge equal:

$$\epsilon_x = \epsilon_y = -\nu\epsilon_z \quad (1)$$

where ϵ = strain in x-, y-, or z-direction, and ν = Poisson's ratio. By definition (Reference 25) effective strain is:

$$\epsilon_{\text{eff}} = \frac{2}{3} (\epsilon_1 - \epsilon_2)^2 + (\epsilon_2 - \epsilon_3)^2 + (\epsilon_3 - \epsilon_1)^2 \quad (2)$$

where 1, 2, and 3 refer to the principal directions. Since the shear strains are zero at the leading edge, the normal strains equal the principal strains. Substituting Equation 1 in Equation 2 gives the effective strain at the leading edge as:

$$\epsilon_{\text{eff}} = \frac{2(1 + \nu)}{3} \epsilon_z \quad (3)$$

3. MINIMUM AND MAXIMUM LONGITUDINAL STRAIN

Results for the five analyzed alloys at the time increment of minimum and maximum leading edge longitudinal strain are shown in Figures 6 and 7, respectively. The complete distribution of temperature and also normal, shear, and effective stresses and strains are shown over the complete mid-chord plane of the wedge. The notation used is conventional elasticity notation with the axes convention as given in Figure 1. The assumption of constant temperature through the thickness of the wedge results in zero y-stress over the mid-chord. For this reason the y-stress plot is not presented. The minimum (largest compressive) longitudinal strain always occurred during heating and the maximum longitudinal strain always occurred during the cooling part of the cycle. These plots were made utilizing the PROUT3 program. These

AFWAL-TR-80-2013

results show the reflective symmetry about mid-span. These plots in addition to those in Figure 5 will be used for further evaluation of various life prediction theories such as strain range partitioning.

SECTION V

SUMMARY OF RESULTS AND CONCLUSIONS

The elastic stress analyses for a double-edge wedge geometry specimen cycled in fluidized beds were determined using conventional three-dimensional finite-element techniques. The analyses were performed as a joint program of the Aero Propulsion Laboratory (AFWAL/POTP) and the National Aeronautics and Space Administration (NASA) Lewis Research Center. IN 100 alloy was analyzed using the NASTRAN computer program with a fine mesh for only one severe heating time increment. The Aero Propulsion Laboratory used the ISO3DQ program with a coarse mesh model for this combination and all other combinations. Five alloys (IN 100, Mar-M 200, Mar-M 302, NASA TAZ-8A, and Rene 80) subjected to the same thermal cycling condition were analyzed. This condition was alternate 3-minute immersions in fluidized beds maintained at 316° and 1088°C (600° and 1990°F). Specific major results are:

(1) The analyses showed the leading edge of the double-edge wedge goes into compression when immersed into the heating bed followed by tension when immersed into the cooling bed. Steep stress and strain gradients occurred during the first 10 seconds of immersion in either bed. For example, 0.48 percent strain was noted for IN 100 alloy during the initial 5 seconds immersion in the heating bed.

(2) The maximum longitudinal strain range (algebraic difference between maximum and minimum longitudinal strain) for the five alloys analyzed varied from 0.53 to 0.82 percent.

(3) The two locations of maximum longitudinal strain range at the leading edge of each wedge were between 0.64 and 2.54 cm (0.25 and 1.00 in.) away from mid-span for the five alloys analyzed. Experimental test data for the alloys that have cracked indicate that the cracks initiated at these locations.

(4) The comparison of the analyses using a fine mesh model (354 elements) and NASTRAN with a coarse mesh model (64 elements) and ISO3DQ showed very good agreement for the single condition checked.

(5) The results from this investigation can be used for further evaluation of various life prediction theories.

TABLE 1
ALLOYS AND CONDITION ANALYZED

Alloy	Fluidized bed cycling condition for all alloys
IN 100 Mar-M 200 Mar-M 302 NASA TAZ-8A Rene 80	Heating bed temperature: 1088 ^o C (1990 ^o F) Cooling bed temperature: 316 ^o C (600 ^o F) Immersion time in each bed: 180 seconds

TABLE 2
TEMPERATURE INDEPENDENT ALLOY PROPERTIES

ALLOY PROPERTIES

Alloy	Poisson's ratio	Density	
		g/cm ³	lb/in ³
IN 100	0.2981	7.750	0.280
Mar-M 200	.3039	8.525	.308
Mar-M 302	.2938	9.217	.333
NASA TAZ-8A	.3166	8.636	.312
Rene 80	.3217	8.166	.295

TABLE 3
TEMPERATURE DEPENDENT ALLOY PROPERTIES

Temperature		IN 100				Mar-M 200				Mar-M 302			
		E ^a		α ^b		E ^a		α ^b		E ^a		α ^b	
°C	°F	$\frac{N}{m^2}$	psi	$\frac{m/m}{°C}$	$\frac{in./in.}{°F}$	$\frac{N}{m^2}$	psi	$\frac{m/m}{°C}$	$\frac{in./in.}{°F}$	$\frac{N}{m^2}$	psi	$\frac{m/m}{°C}$	$\frac{in./in.}{°F}$
260	500	203×10 ⁹	29.4×10 ⁶	13.0×10 ⁻⁶	7.25×10 ⁻⁶	210×10 ⁹	30.4×10 ⁶	12.2×10 ⁻⁶	6.75×10 ⁻⁶	231×10 ⁹	33.5×10 ⁶	12.8×10 ⁻⁶	7.1×10 ⁻⁶
316	600	199	28.9	13.1	7.3	207	30.0	12.4	6.9	226	32.8	13.0	7.2
371	700	197	28.6	13.3	7.4	205	29.7	12.6	7.0	222	32.2	13.1	7.3
427	800	194	28.1	13.5	7.5	201	29.2	12.8	7.1	219	31.8	13.3	7.4
482	900	191	27.7	13.7	7.6	199	28.8	13.0	7.2	212	30.8	13.5	7.5
538	1000	187	27.1	13.9	7.7	194	28.2	13.1	7.3	210	30.4	13.7	7.6
593	1100	184	26.7	14.0	7.8	191	27.7	13.3	7.4	203	29.4	13.9	7.7
649	1200	180	26.1	14.4	8.0	188	27.2	13.5	7.5	199	28.8	14.0	7.8
704	1300	177	25.6	14.6	8.1	182	26.4	13.7	7.6	192	27.9	14.2	7.9
760	1400	173	25.1	14.9	8.3	178	25.8	14.0	7.8	188	27.2	14.4	8.0
816	1500	168	24.3	15.4	8.55	173	25.1	14.2	7.9	182	26.4	14.6	8.1
871	1600	162	23.5	15.8	8.8	168	24.4	14.8	8.2	177	25.6	14.9	8.3
927	1700	157	22.7	16.4	9.1	163	23.7	15.1	8.4	172	24.9	15.3	8.5
982	1800	151	21.9	16.7	9.3	158	22.9	15.8	8.8	167	24.2	15.7	8.7
1038	1900	145	21.1	17.5	9.7	152	22.1	16.7	9.3	160	23.2	16.0	8.9
1093	2000	139	20.2	18.2	10.1	147	21.3	17.6	9.8	155	22.5	16.6	9.2

Temperature		NASA TAZ-8A				Rene 80			
		E ^a		α ^b		E ^a		α ^b	
°C	°F	$\frac{N}{m^2}$	psi	$\frac{m/m}{°C}$	$\frac{in./in.}{°F}$	$\frac{N}{m^2}$	psi	$\frac{m/m}{°C}$	$\frac{in./in.}{°F}$
260	500	202×10 ⁹	29.3×10 ⁶	12.1×10 ⁻⁶	6.7×10 ⁻⁶	188×10 ⁹	27.3×10 ⁶	12.4×10 ⁻⁶	6.9×10 ⁻⁶
316	600	201	29.1	12.1	6.7	186	27.0	12.6	7.0
371	700	199	28.9	12.2	6.8	184	26.7	12.8	7.1
427	800	198	28.7	12.4	6.9	181	26.3	13.0	7.2
482	900	197	28.5	12.6	7.0	179	26.0	13.1	7.3
538	1000	194	28.2	12.8	7.1	174	25.3	13.3	7.4
593	1100	192	27.9	12.8	7.1	172	24.9	13.5	7.5
649	1200	190	27.5	13.0	7.2	168	24.3	13.7	7.6
704	1300	187	27.1	13.1	7.3	164	23.8	14.0	7.8
760	1400	183	26.5	13.3	7.4	159	23.1	14.4	8.0
816	1500	178	25.8	13.5	7.5	154	22.3	14.8	8.2
871	1600	168	24.3	13.9	7.7	147	21.3	15.1	8.4
927	1700	146	21.2	14.2	7.9	139	20.2	15.7	8.7
982	1800	139	20.2	14.6	8.1	126	18.3	16.2	9.0
1038	1900	133	19.3	14.9	8.3	122	17.7	16.7	9.3
1093	2000	128	18.5	15.3	8.5	114	16.5	17.5	9.7

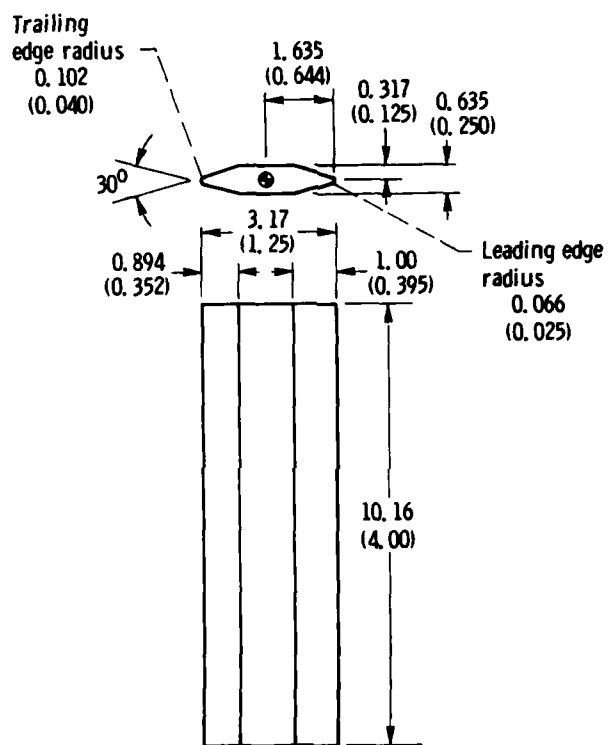
^a Modulus of elasticity.

^b Mean coefficient of thermal expansion from room temperature to indicated temperature.

TABLE 4
TEMPERATURE VARIATION ALONG SPAN

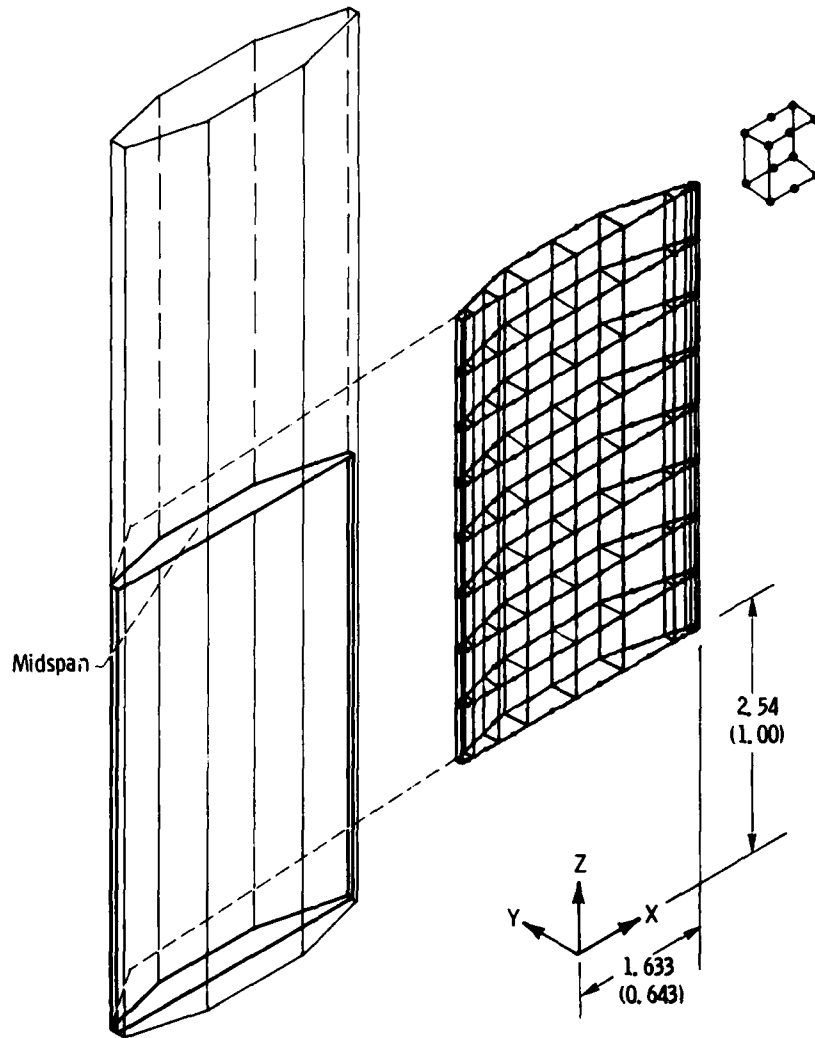
[$T_{x,z} = T_{x,ms} (Az^2 + Bz + C)$, where $T_{x,z}$ is the temperature at any x, z coordinate (see fig. 1), $T_{x,ms}$ is the temperature at the x coordinate at midspan, and z is the span coordinate; all temperatures in $^{\circ}F$ ($F = 9/5 C + 32$).]

Time increment, sec	Heating bed			Cooling bed		
	A	B	C	A	B	C
0	-0.00870	0.0517	0.9205	-0.00666	0.03957	0.9427
3	.04401	-.2614	1.3891	-.01775	.1055	.8447
6	.03739	-.2221	1.3290	-.02384	.1416	.7911
9	.03688	-.2191	1.3372	-.02548	.1514	.7786
12	.03806	-.2261	1.3344	-.02731	.1622	.7622
15	.03695	-.2195	1.3300	-.02889	.1716	.7480
30	.02758	-.1638	1.2504	-.03047	.1810	.7338
45	.01769	-.1051	1.1630	-.03141	.1866	.7224
60	.01432	-.08506	1.1324	-.03442	.2044	.6905
75	.01006	-.05978	1.0934	-.03265	.1939	.7093
90	.00833	-.04948	1.0791	-.02867	.1703	.7440
105	.00557	-.03311	1.0528	-.02445	.1452	.7843
120	.00627	-.03722	1.0571	-.02276	.1352	.7981
135	.00440	-.02614	1.0415	-.01876	.1142	.8323
150	.00371	-.02205	1.0357	-.01533	.09107	.8622
165	.00297	-.01762	1.0285	-.01278	.07593	.8832
180	.00262	-.01553	1.0243	-.01212	.07198	.8876



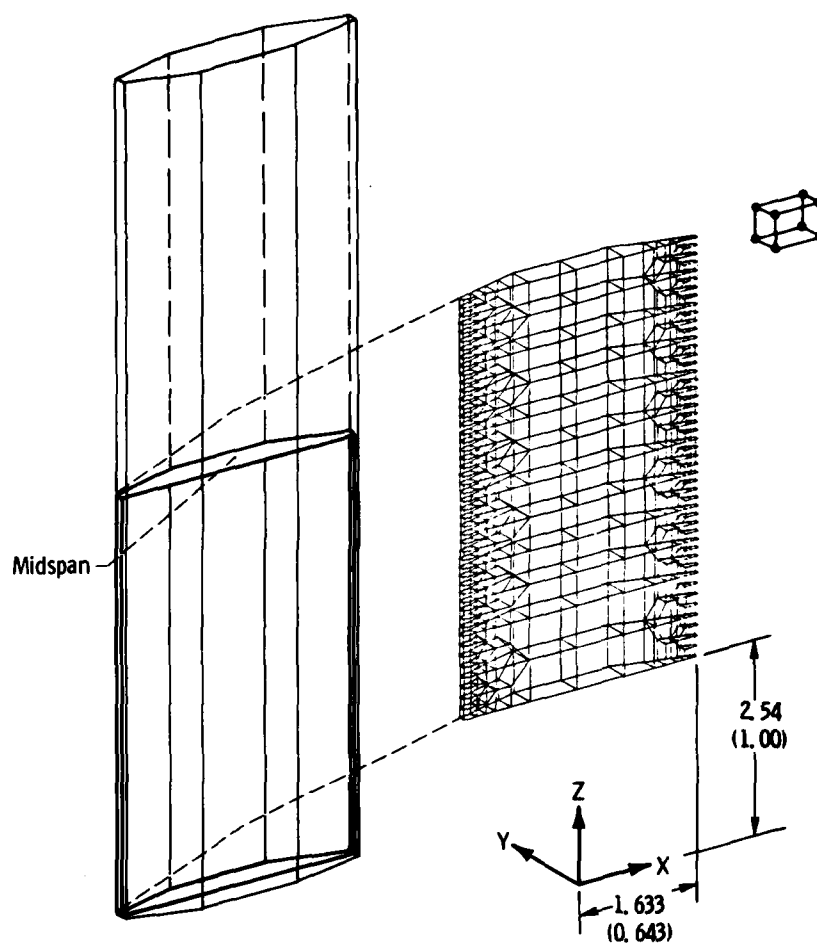
(a) Wedge geometry.

Figure 1. - Double-edge wedge. (All dimensions in cm (in.) unless indicated otherwise.)



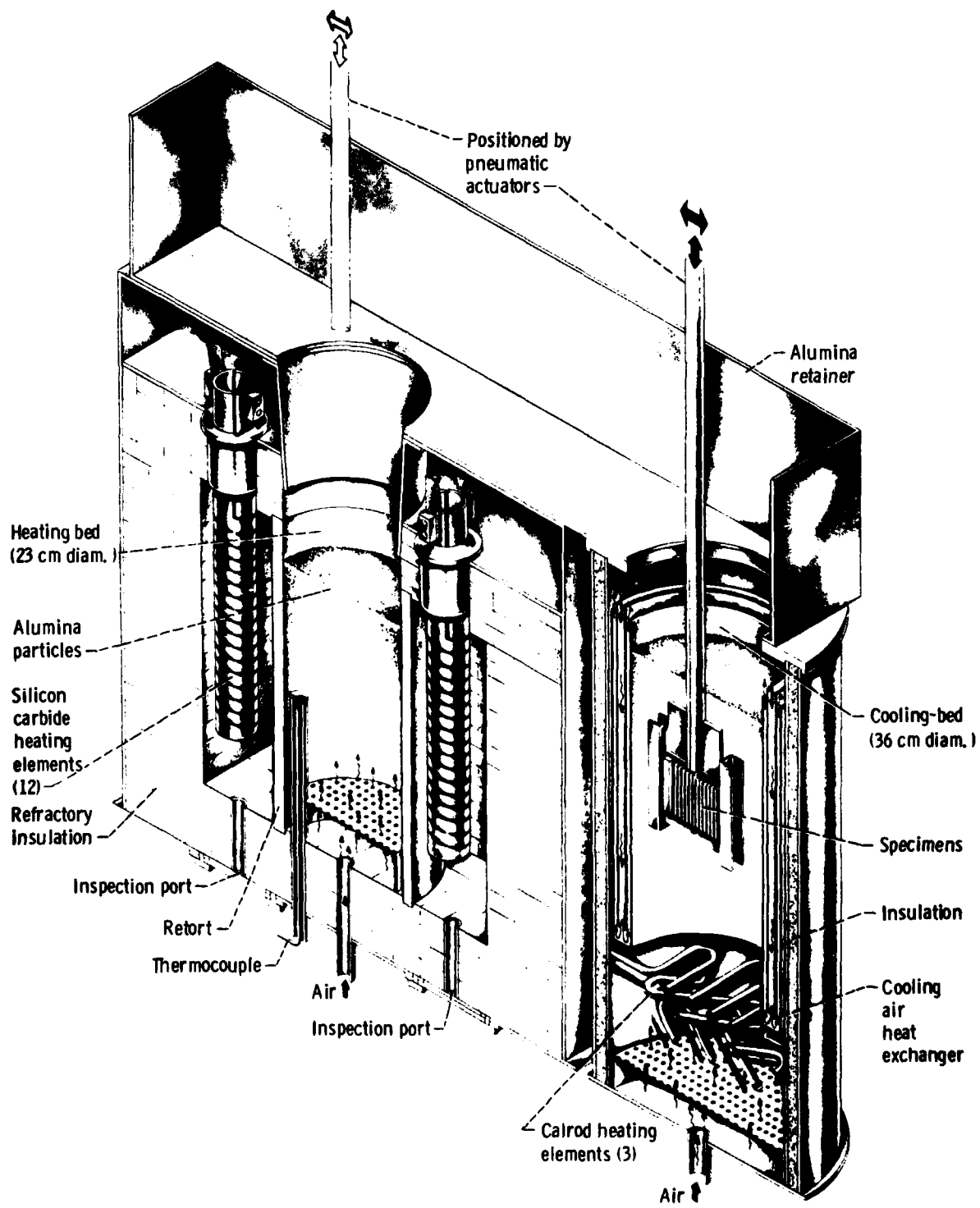
(b) Model and typical element used for ISO3DQ analysis with coordinate convention.

Figure 1. - Continued.



(c) Model and typical element used for NASTRAN analysis with coordinate convention.

Figure 1. - Concluded.



CD-11823-34

CS-73743

Figure 2. - Schematic of fluidized bed test facility.

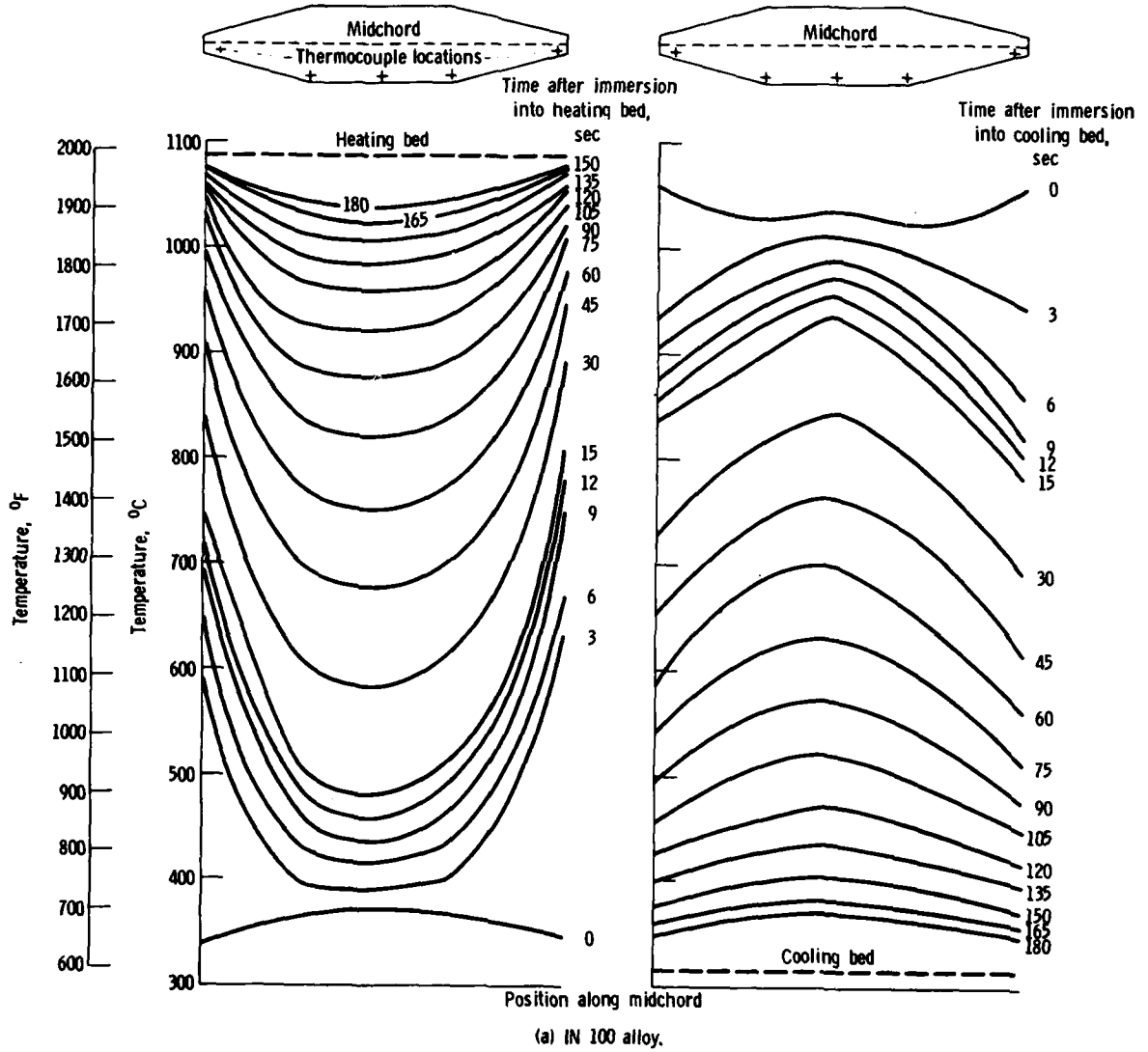
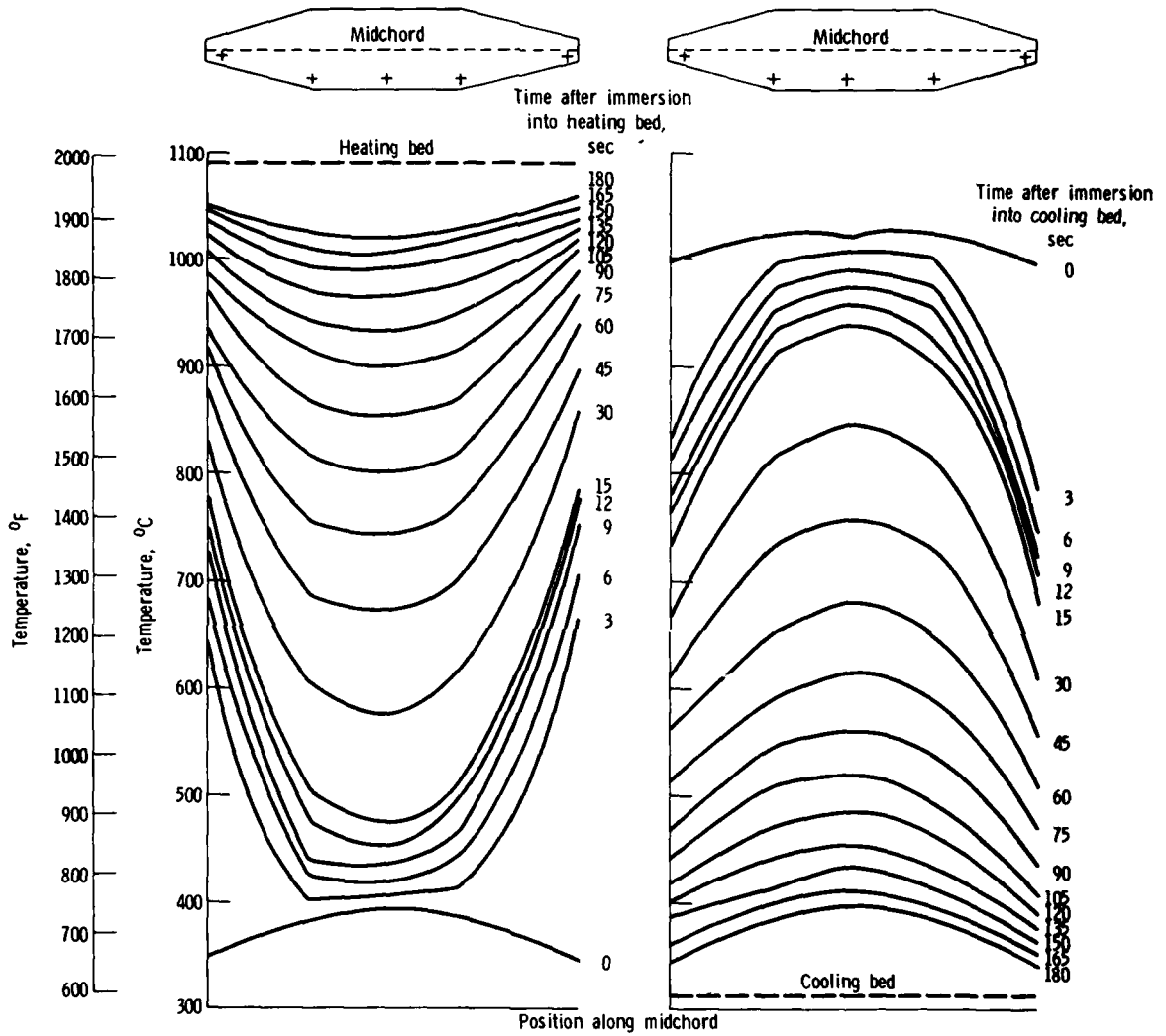
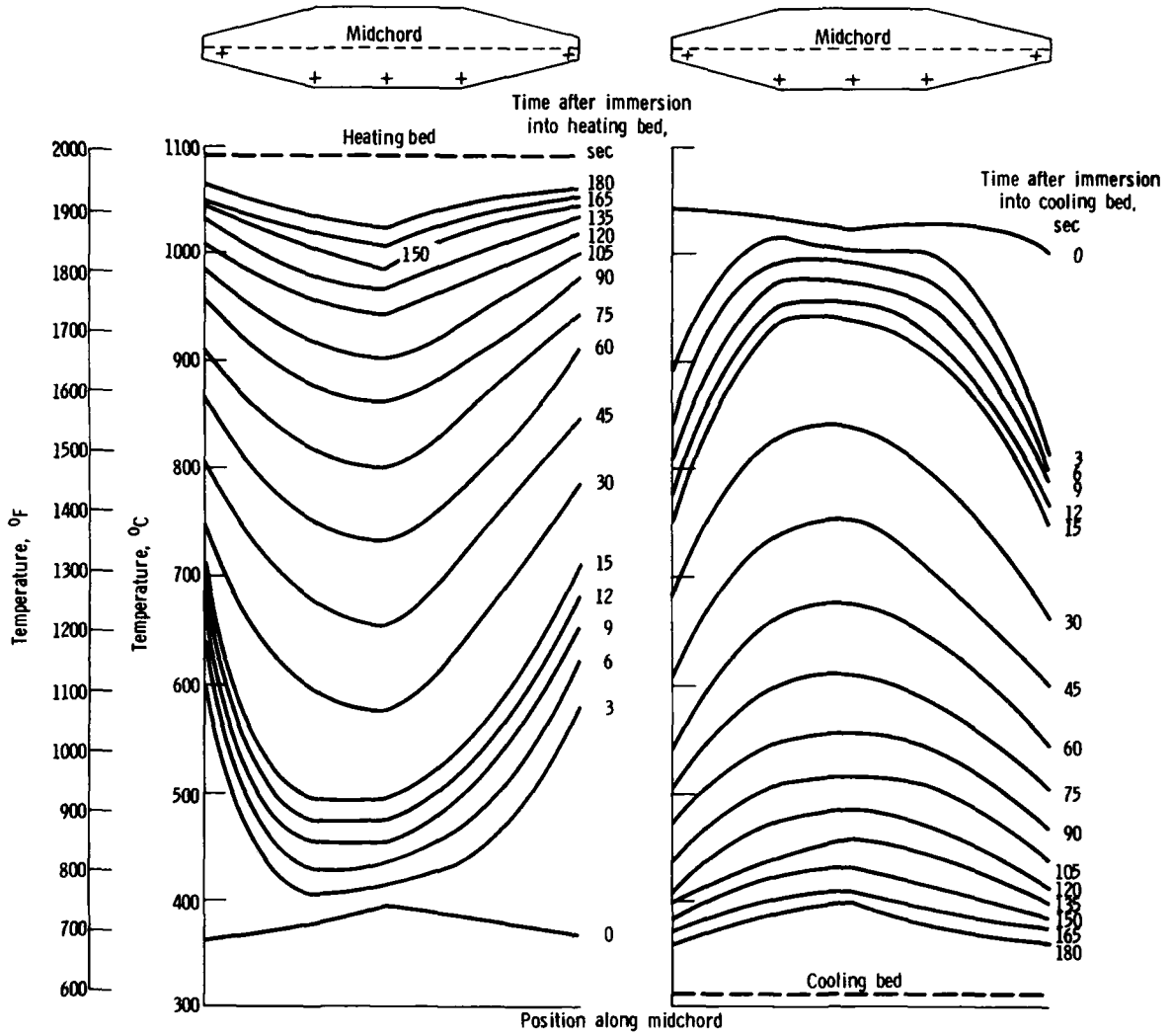


Figure 3. - Temperature of midchord at midspan at various times after immersion into the fluidized beds.



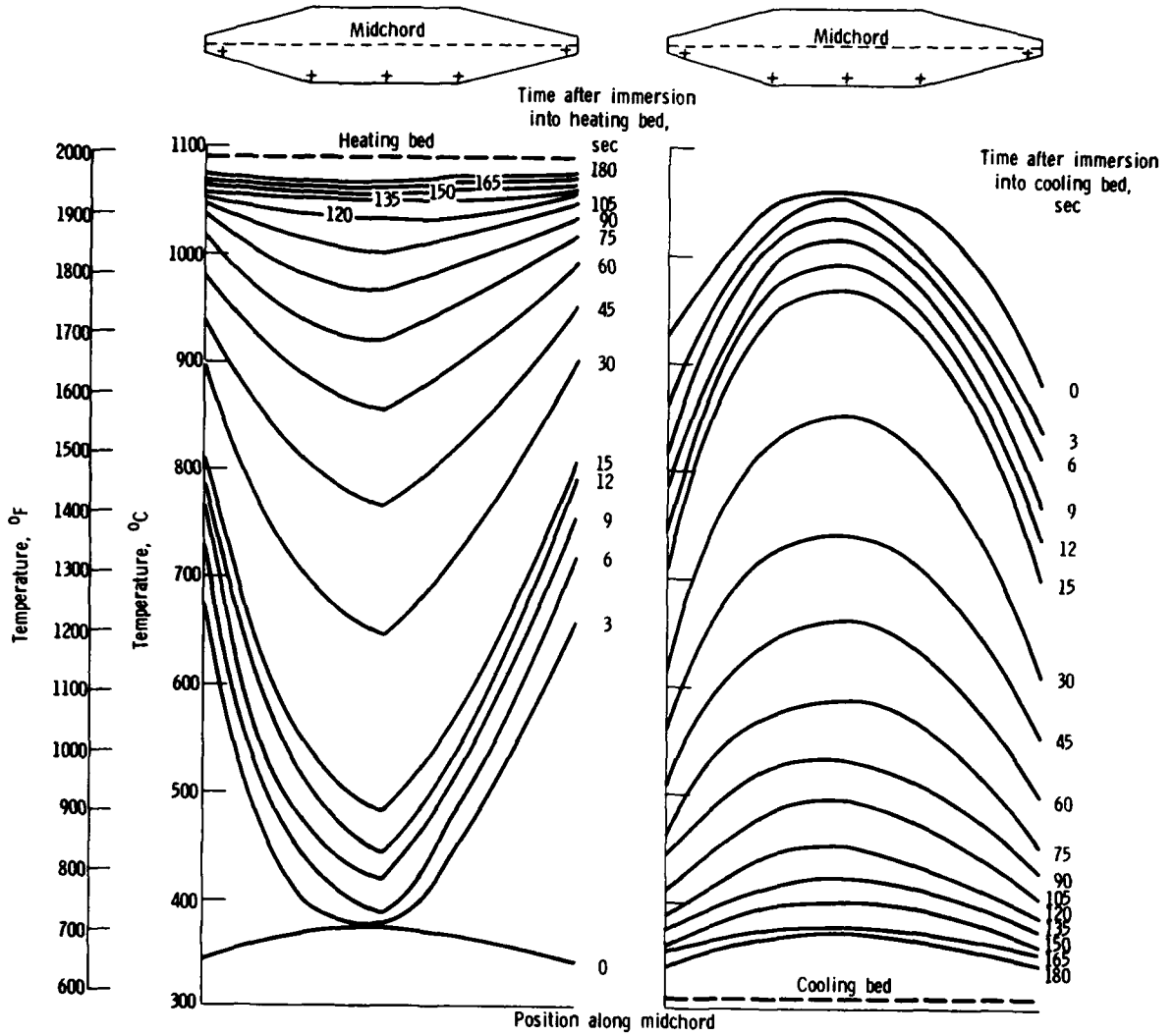
(b) Mar-M 200 alloy.

Figure 3. - Continued.



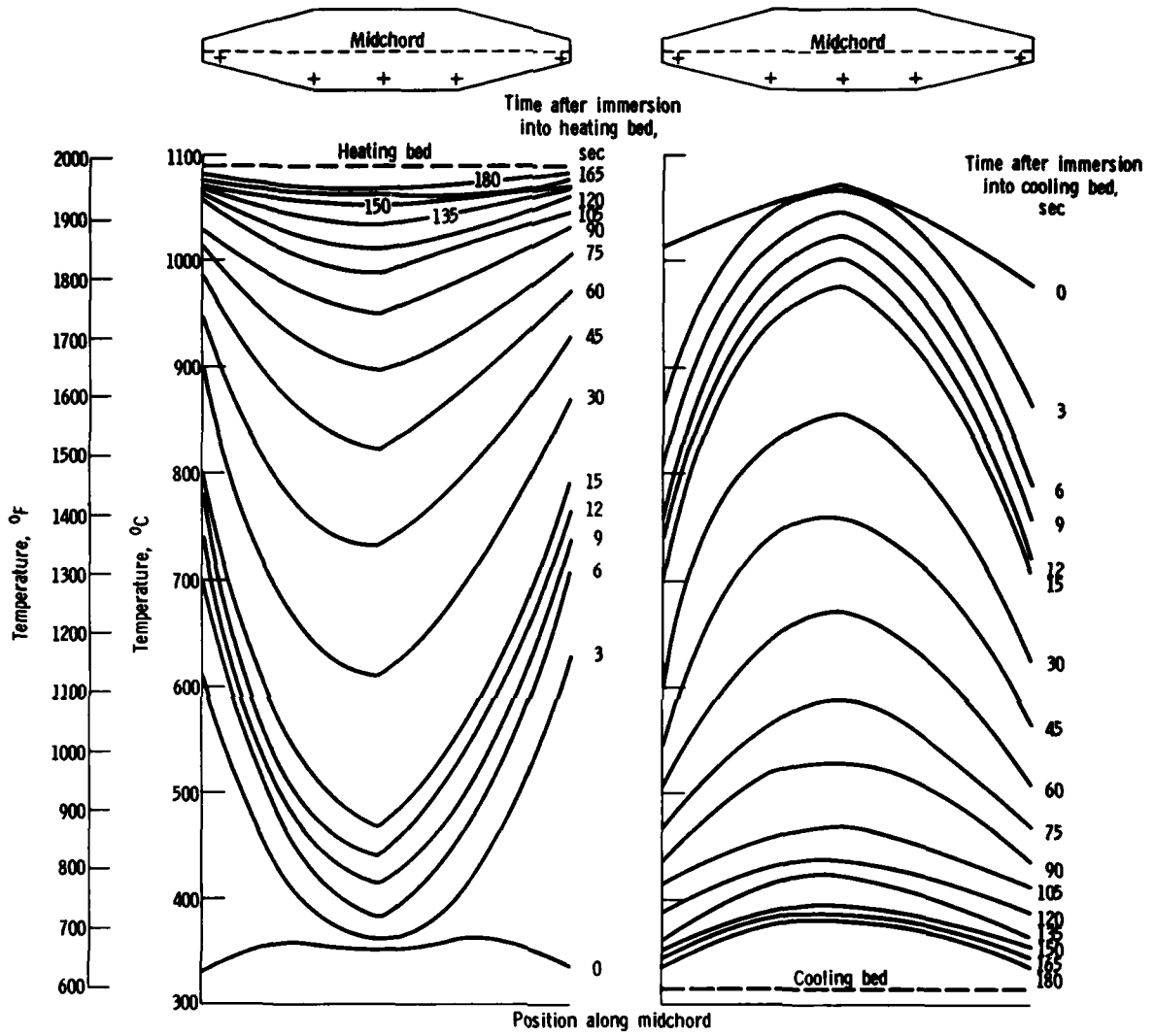
(c) Mar-M 302 alloy.

Figure 3. - Continued.



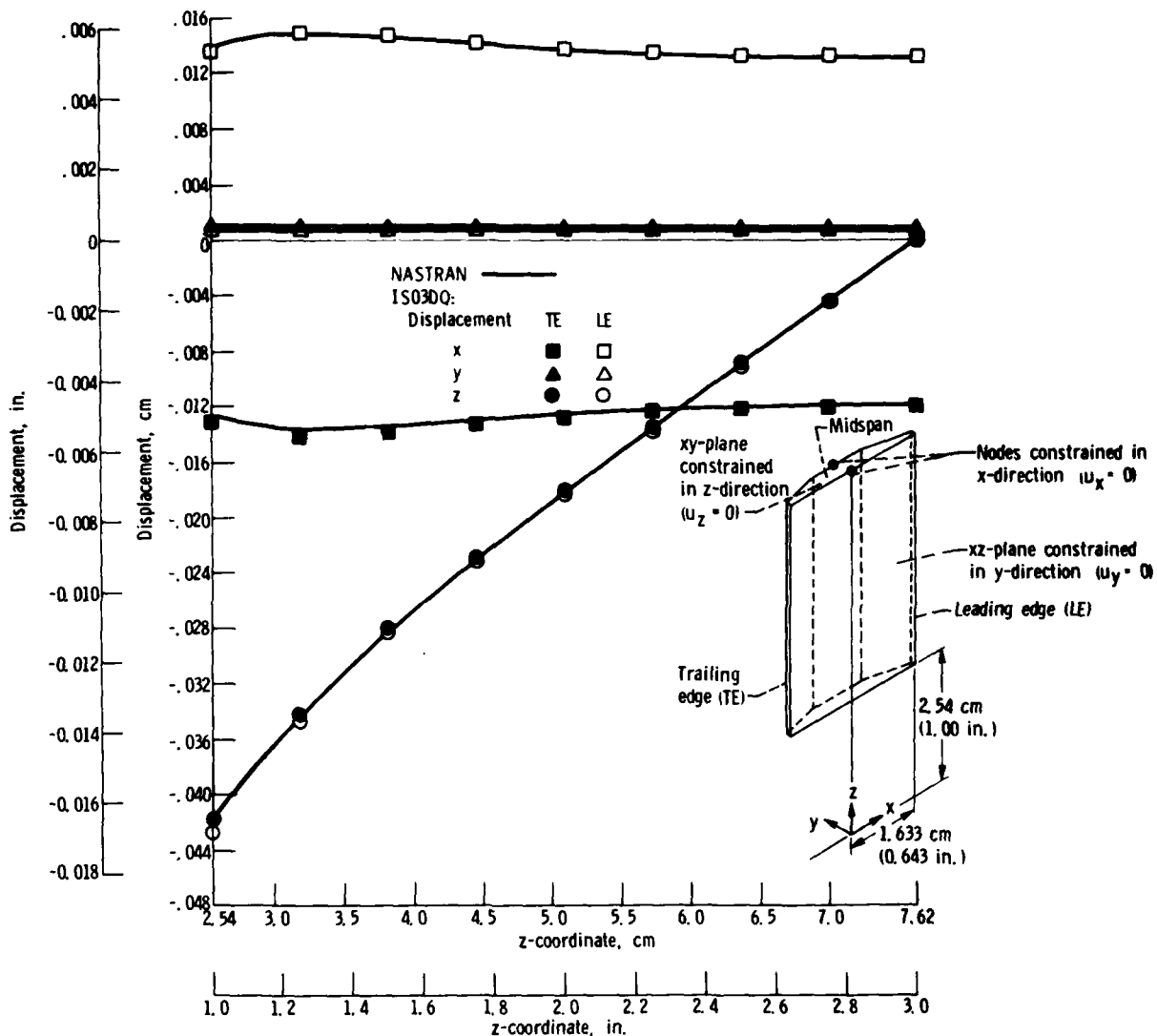
(d) NASA TAZ-8A alloy.

Figure 3 - Continued.



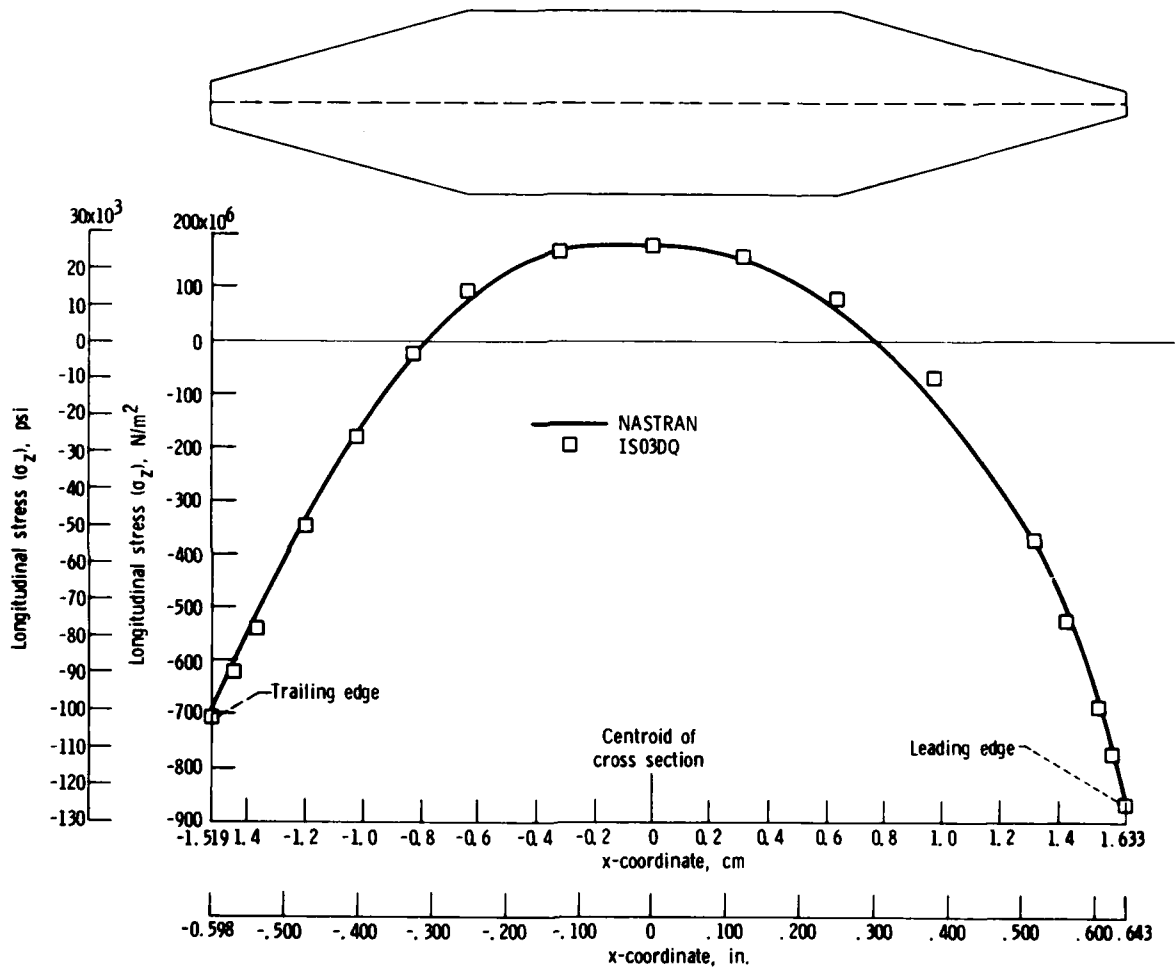
(e) Rene' 80 alloy.

Figure 3 - Concluded.



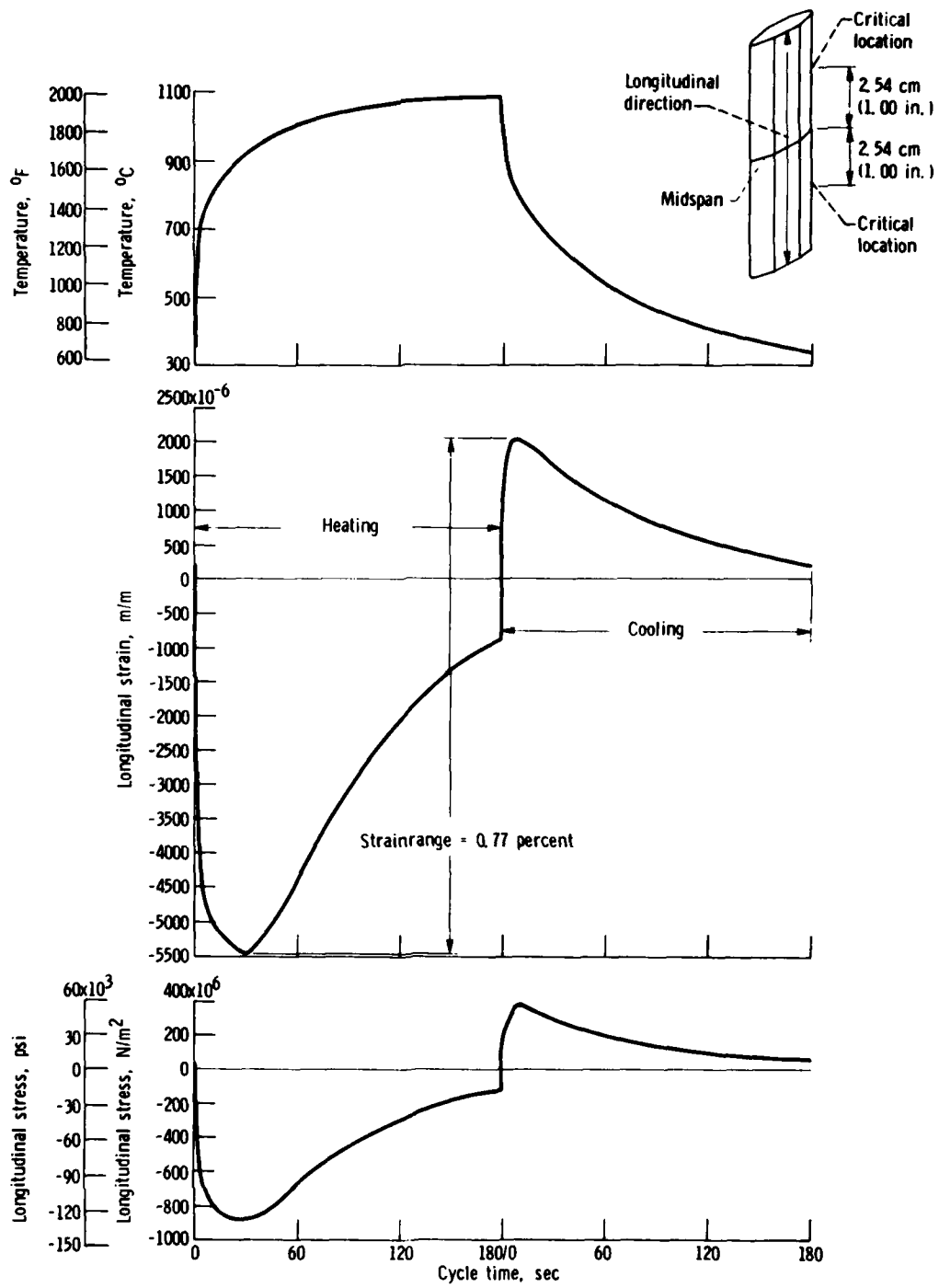
(a) Normal displacements.

Figure 4 - Comparisons determined by using IS0300 and NASTRAN computer programs (using the models in fig. 1) for IN 100 alloy after 15 seconds heating in the 1088° C (1990° F) fluidized bed.



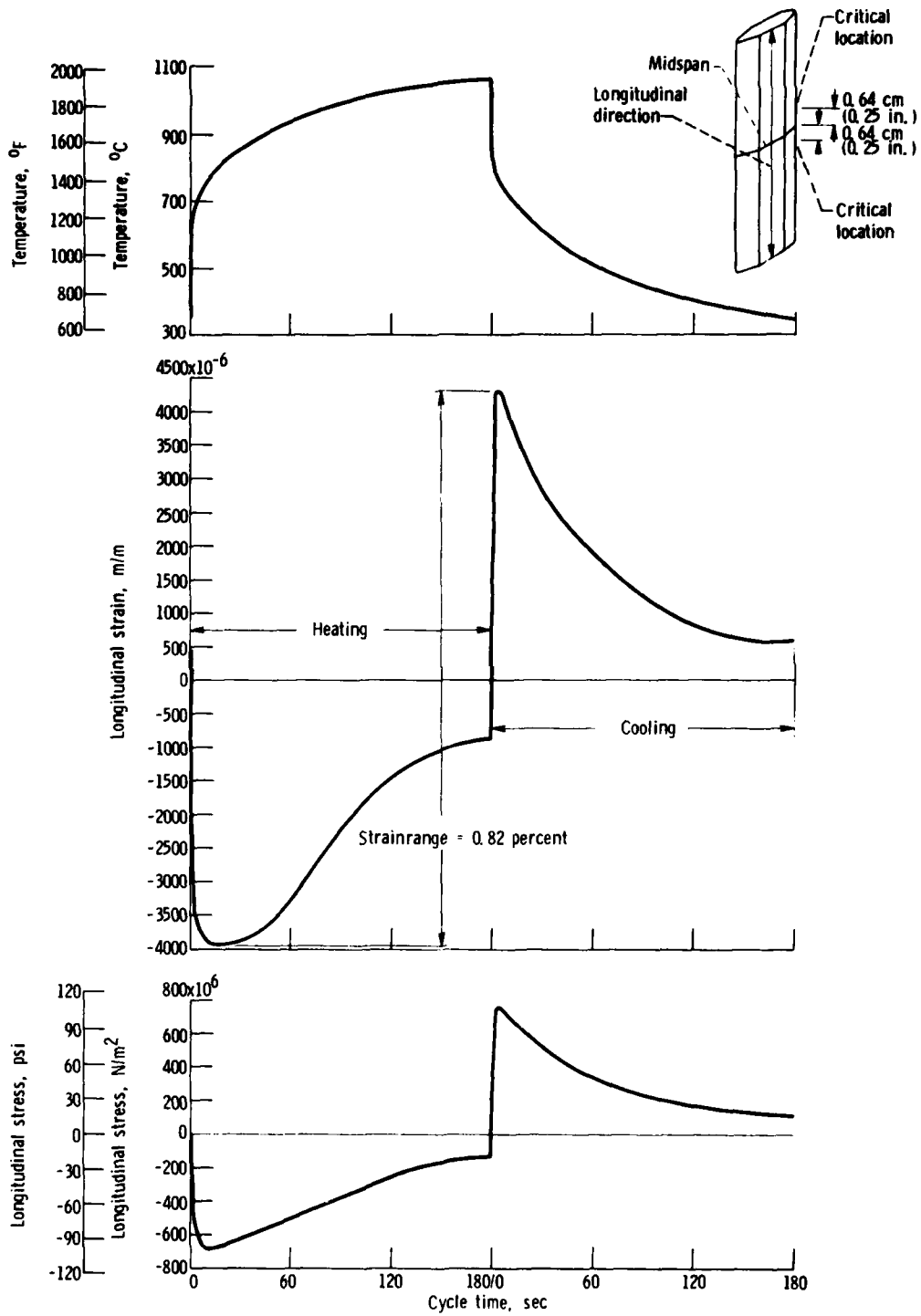
(b) Longitudinal stress (σ_z) along midchord at $z = 5.08$ cm ($z = 2.00$ in.).

Figure 4. - Concluded.



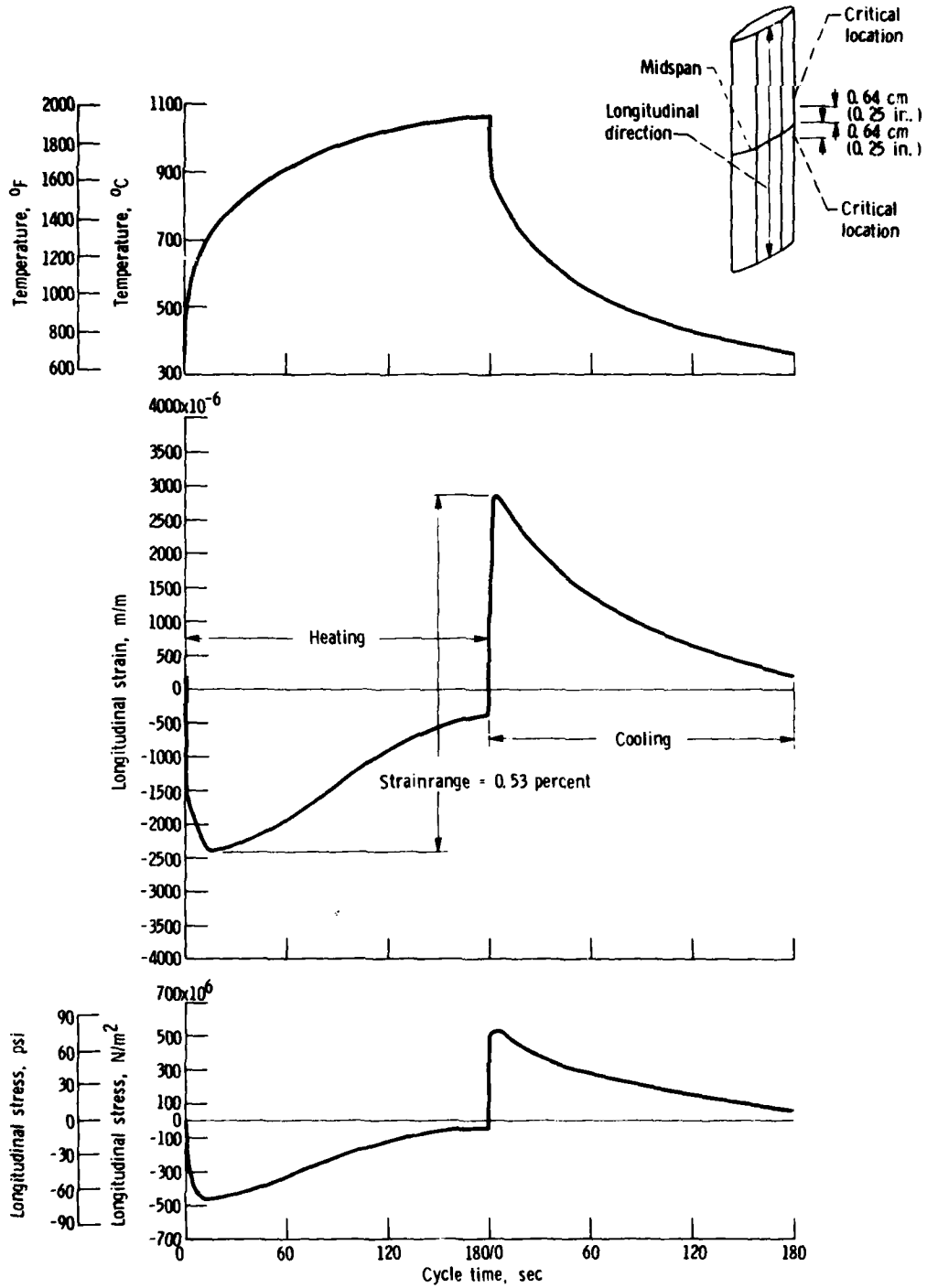
(a) IN 100 alloy.

Figure 5. - Temperature, longitudinal strain, and longitudinal stress at critical locations during a typical fluidized bed cycle.



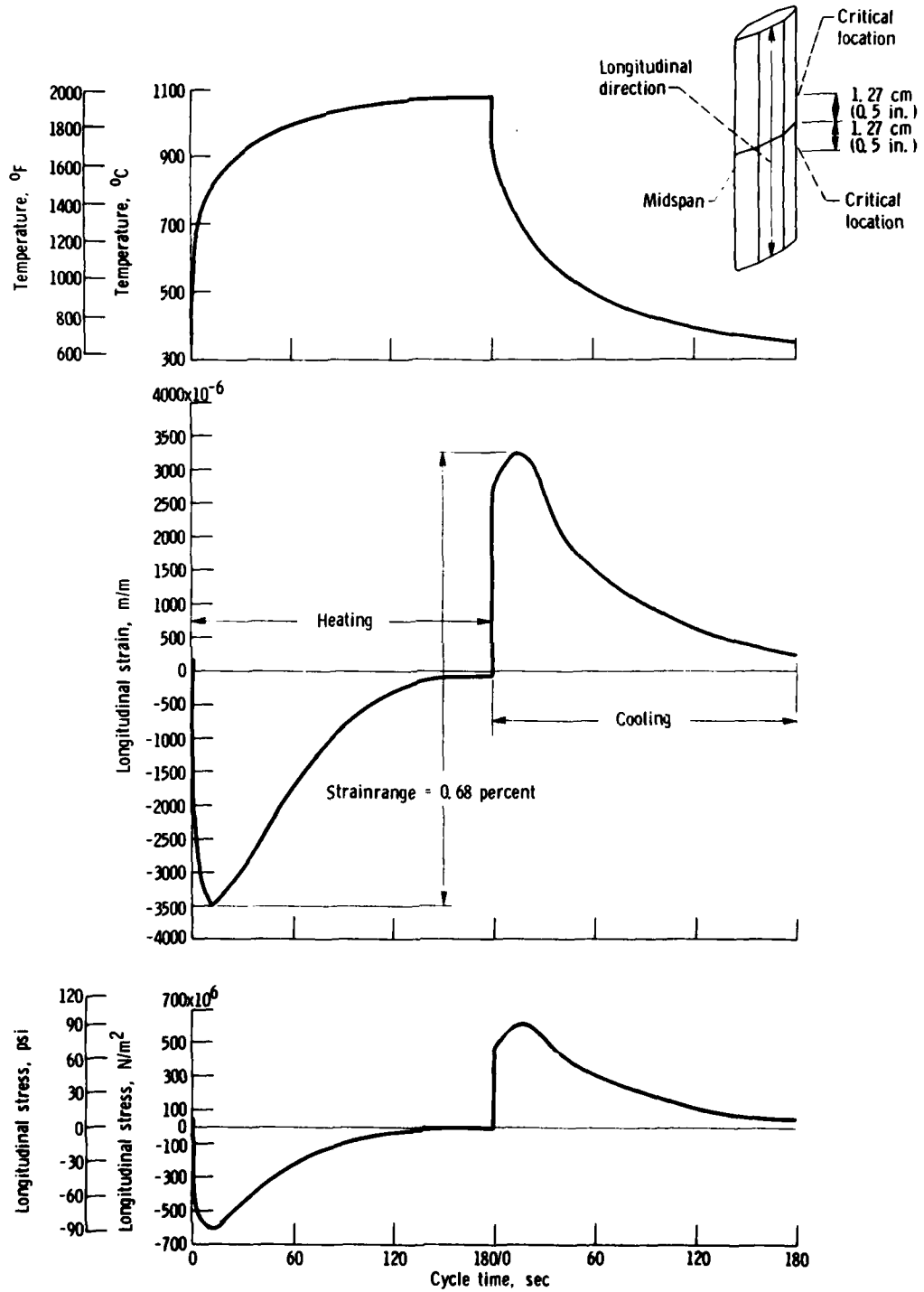
(b) Mar-M 200 alloy.

Figure 5. - Continued.



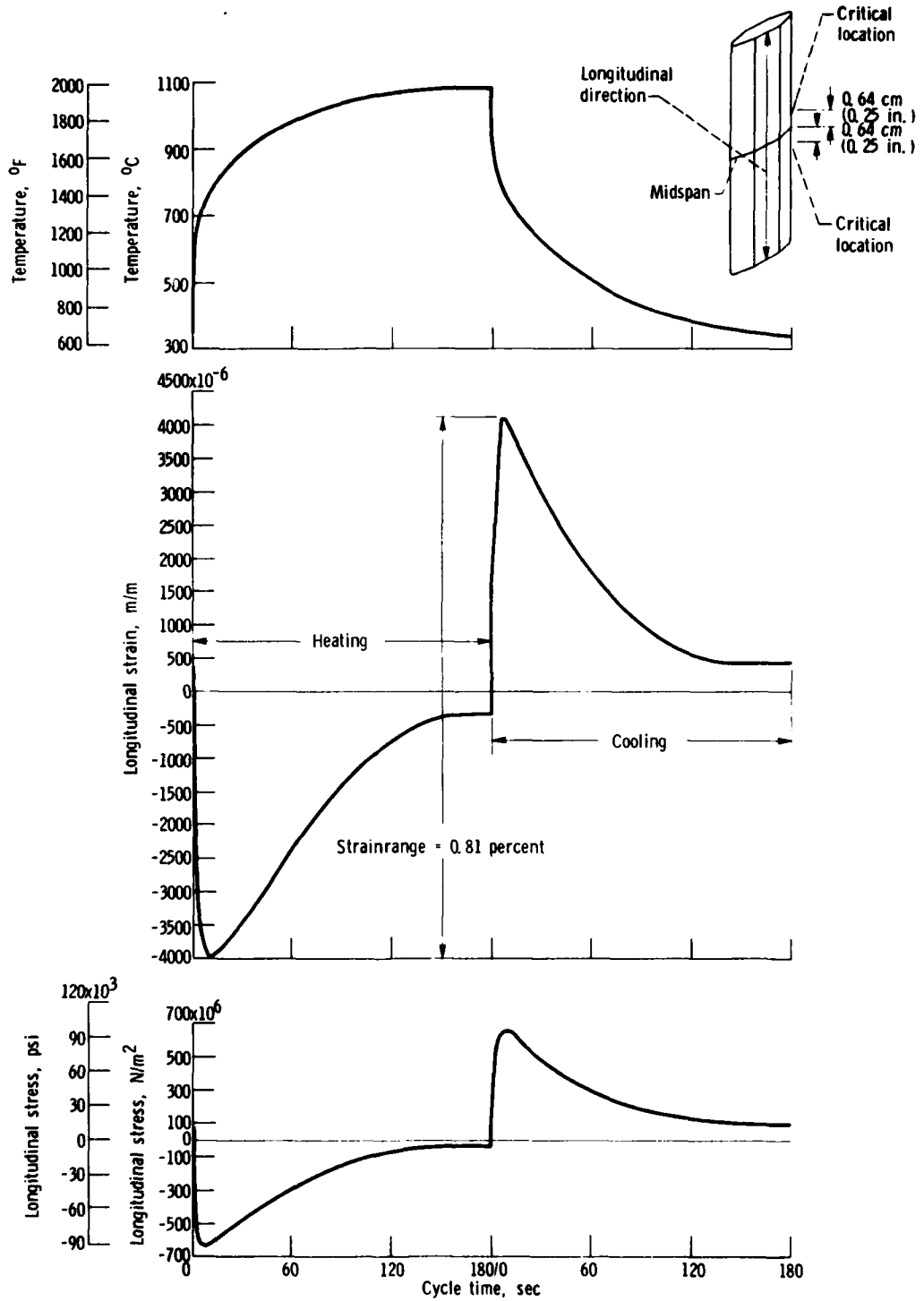
(c) Mar-M 302 alloy.

Figure 5. - Continued.



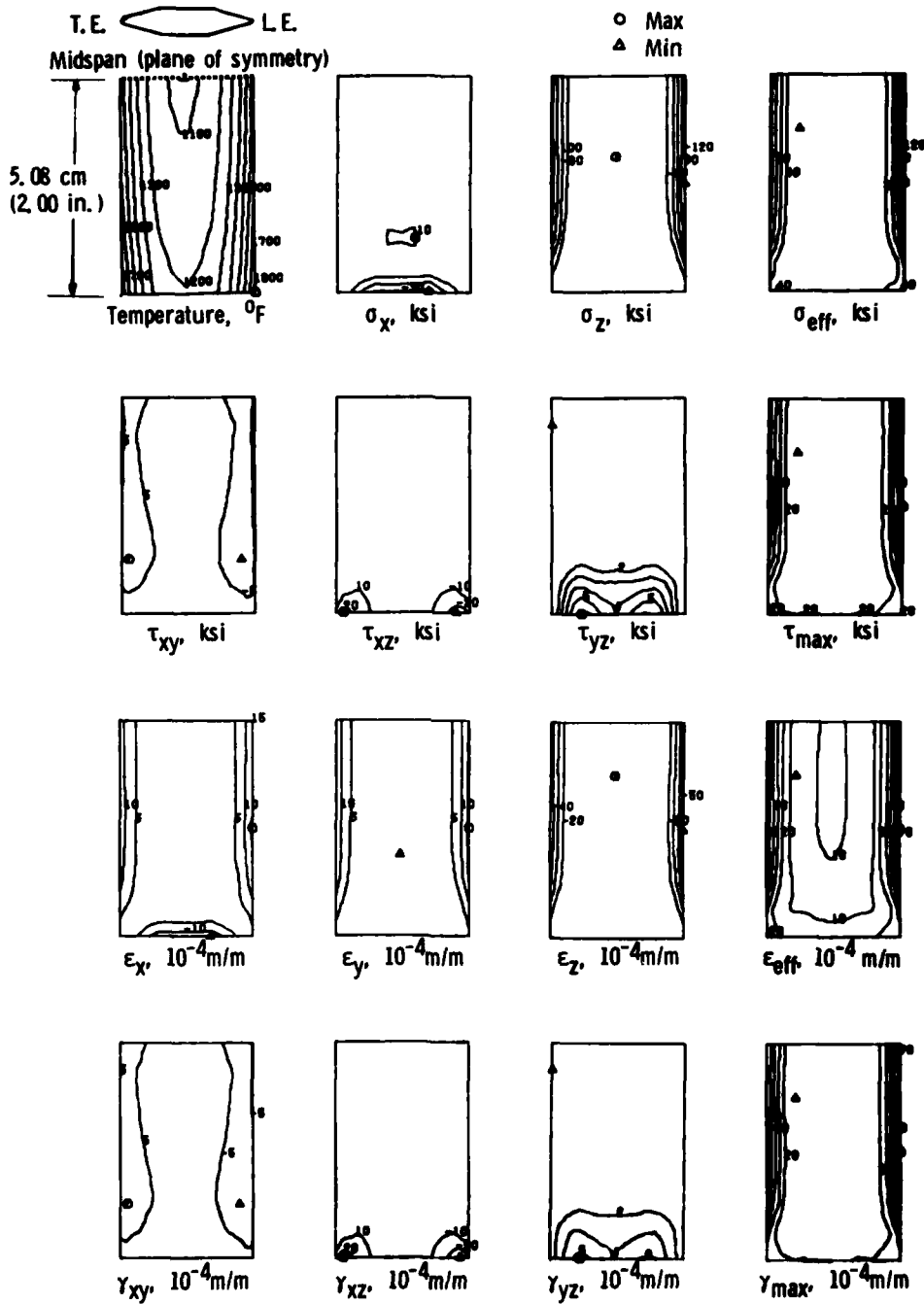
(d) NASA TAZ-8A alloy.

Figure 5. - Continued.



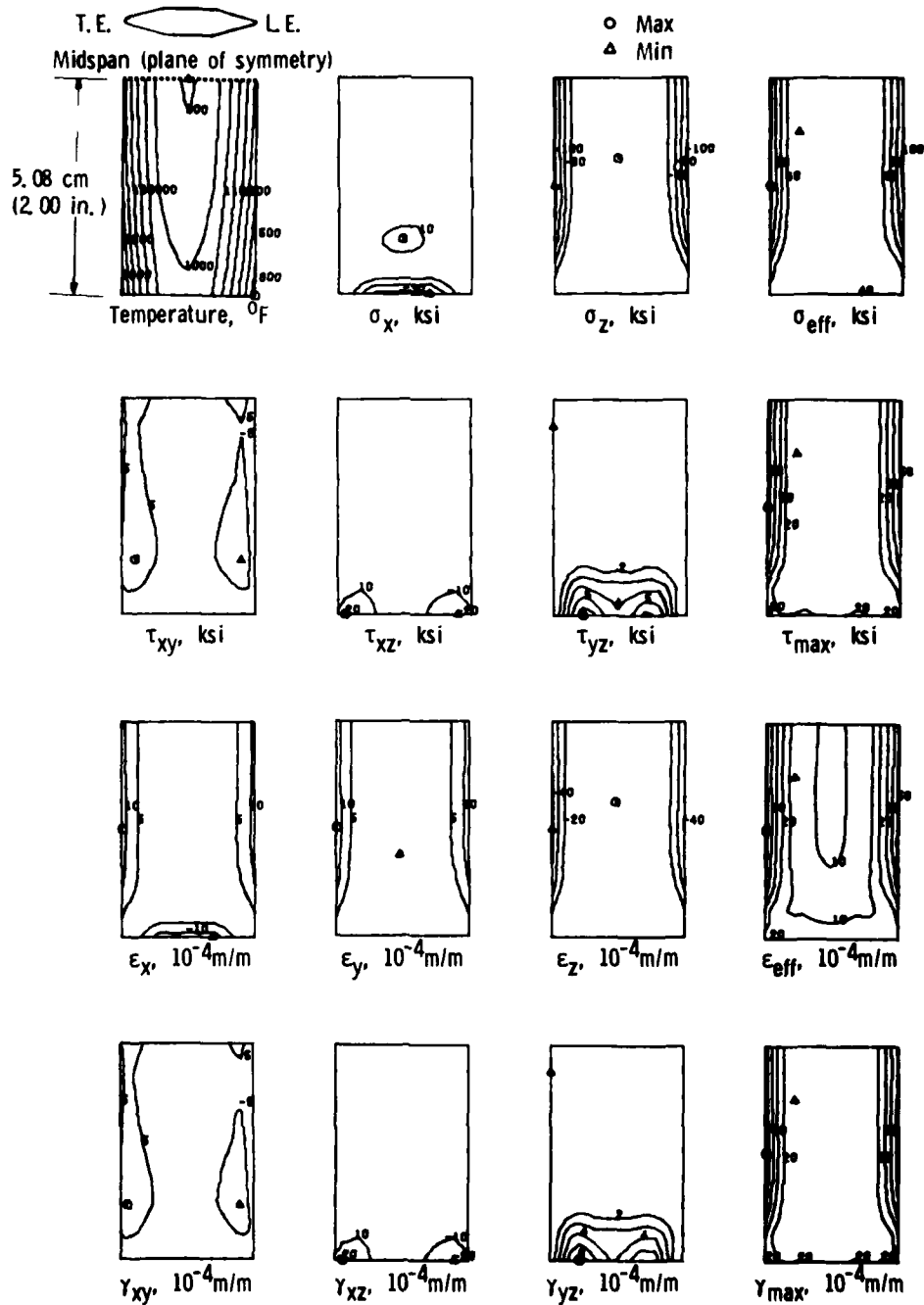
(e) Rene' 80 alloy.

Figure 5. - Concluded.



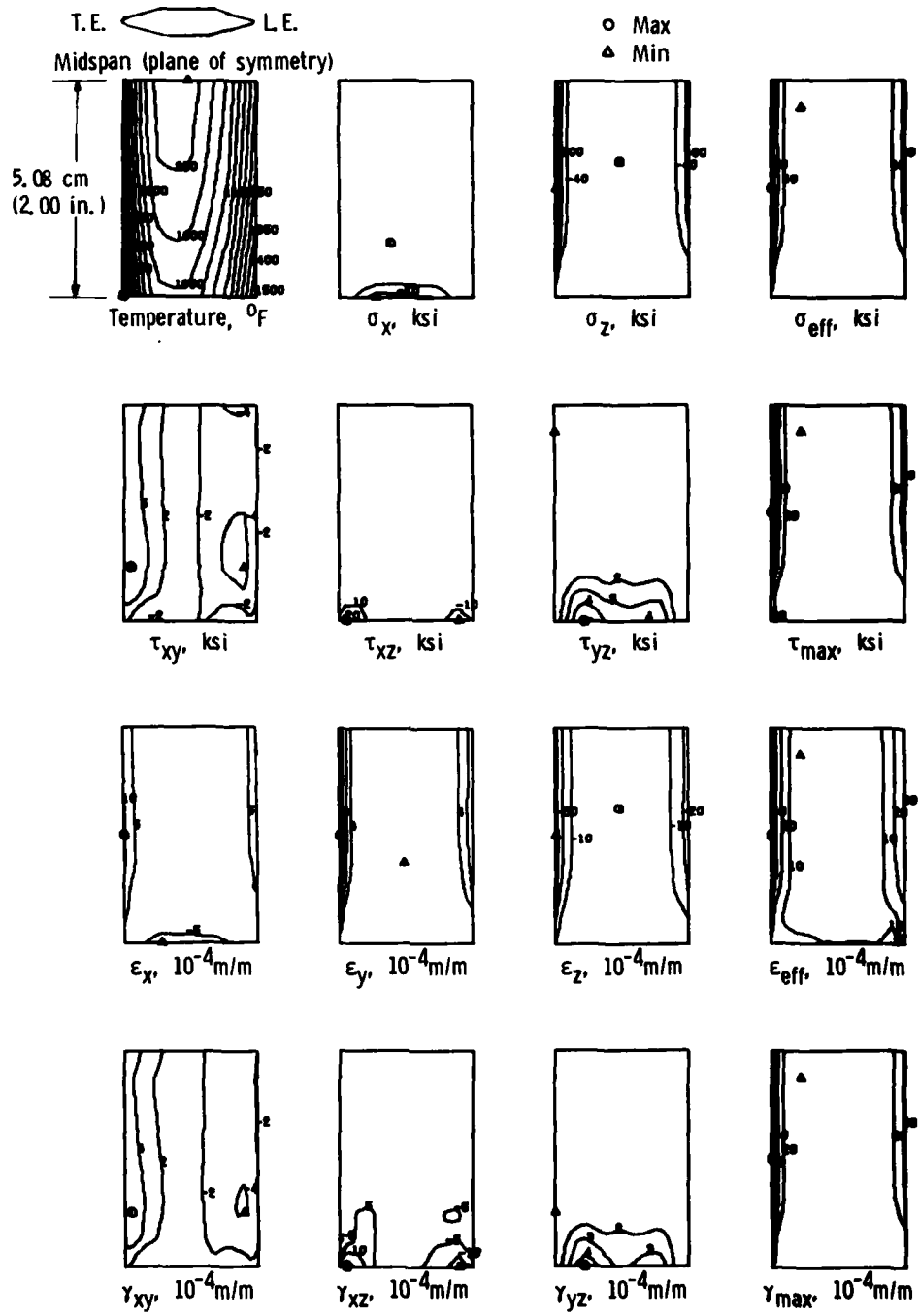
(a) IN 100 alloy after 30 seconds immersion in the heating bed.

Figure 6. - Temperature, stress, and strain distribution of midchord at time of minimum leading edge longitudinal strain. ($F = 9/5 C + 32$)(1 ksi = 6.89×10^6 N/m²).



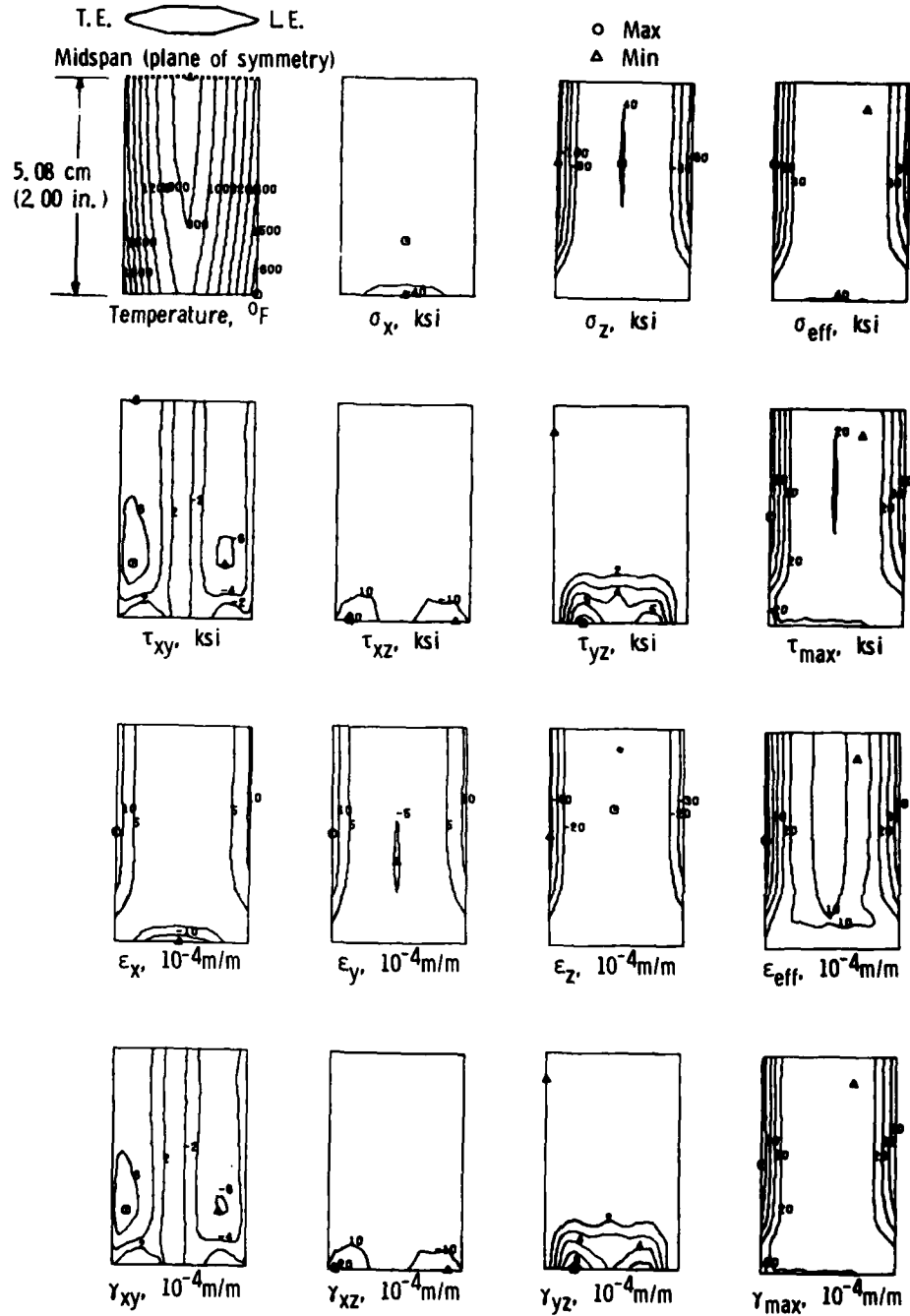
(b) Mar-M 200 alloy after 15 seconds immersion in the heating bed.

Figure 6. - Continued.



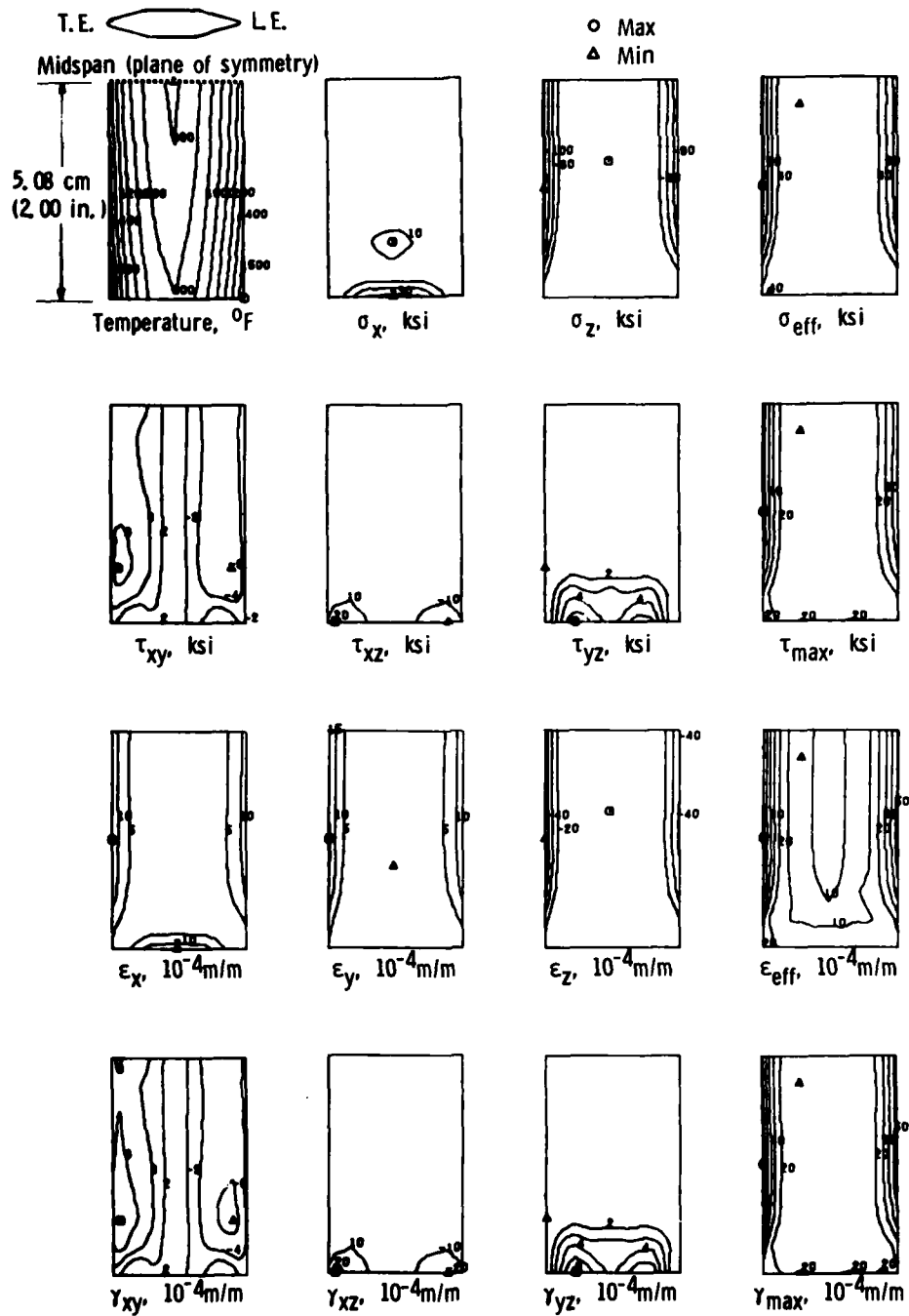
(c) Mar-M 302 alloy after 15 seconds immersion in the heating bed.

Figure 6. - Continued.



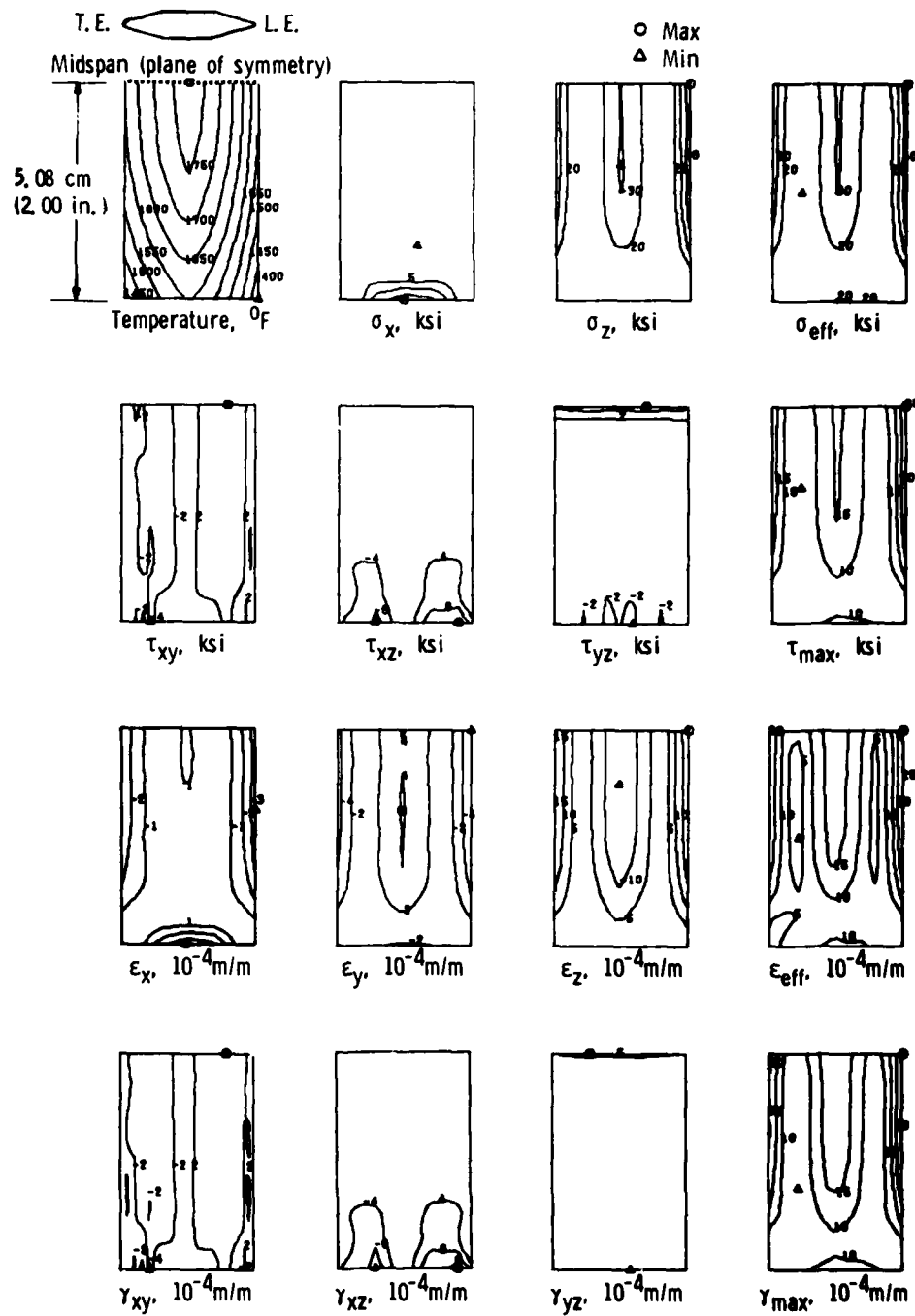
(d) NASA TAZ-8A alloy after 12 seconds immersion in the heating bed.

Figure 6. - Continued.



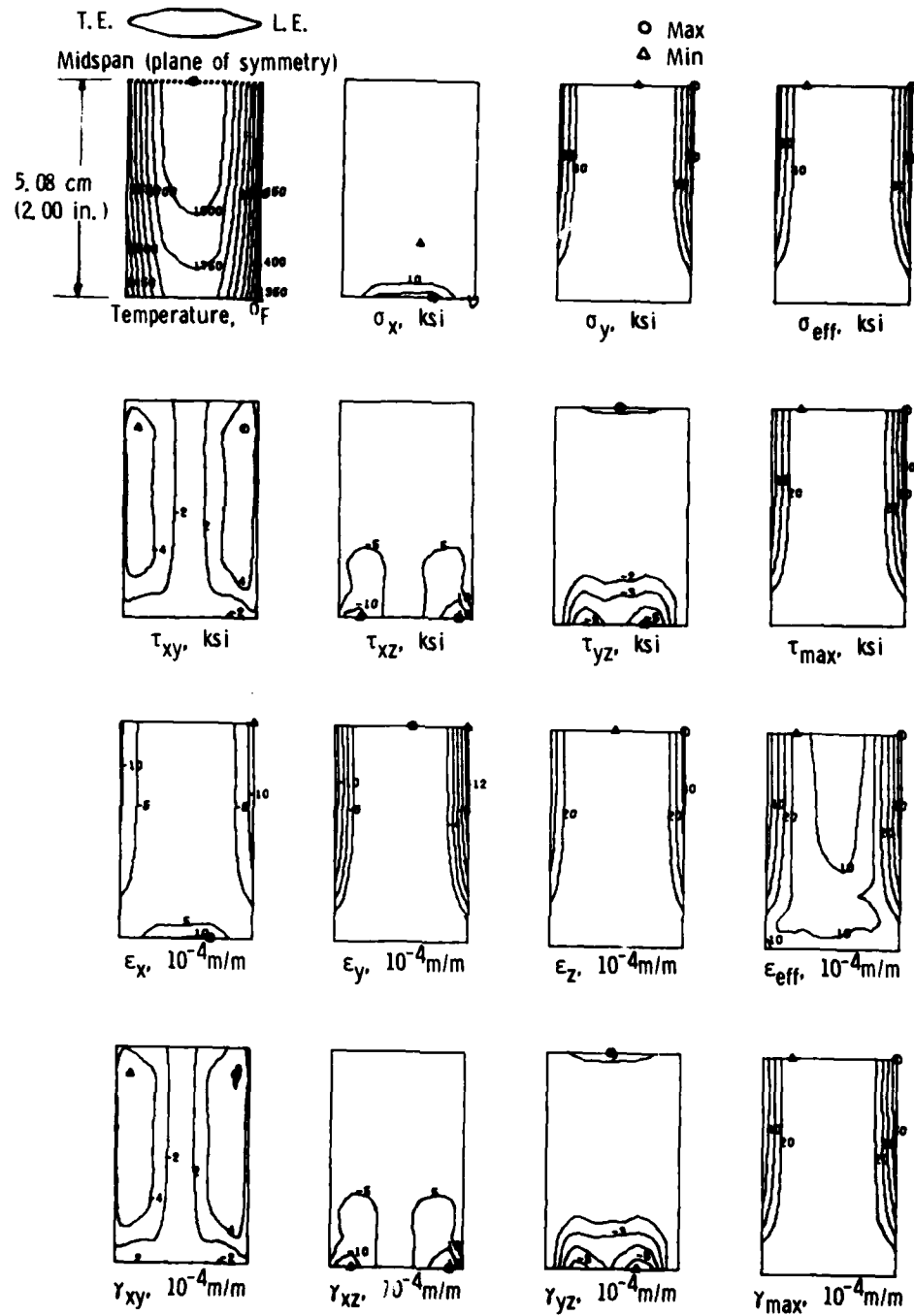
(e) Rene 80 alloy after 9 seconds immersion in the heating bed.

Figure 6. - Concluded.



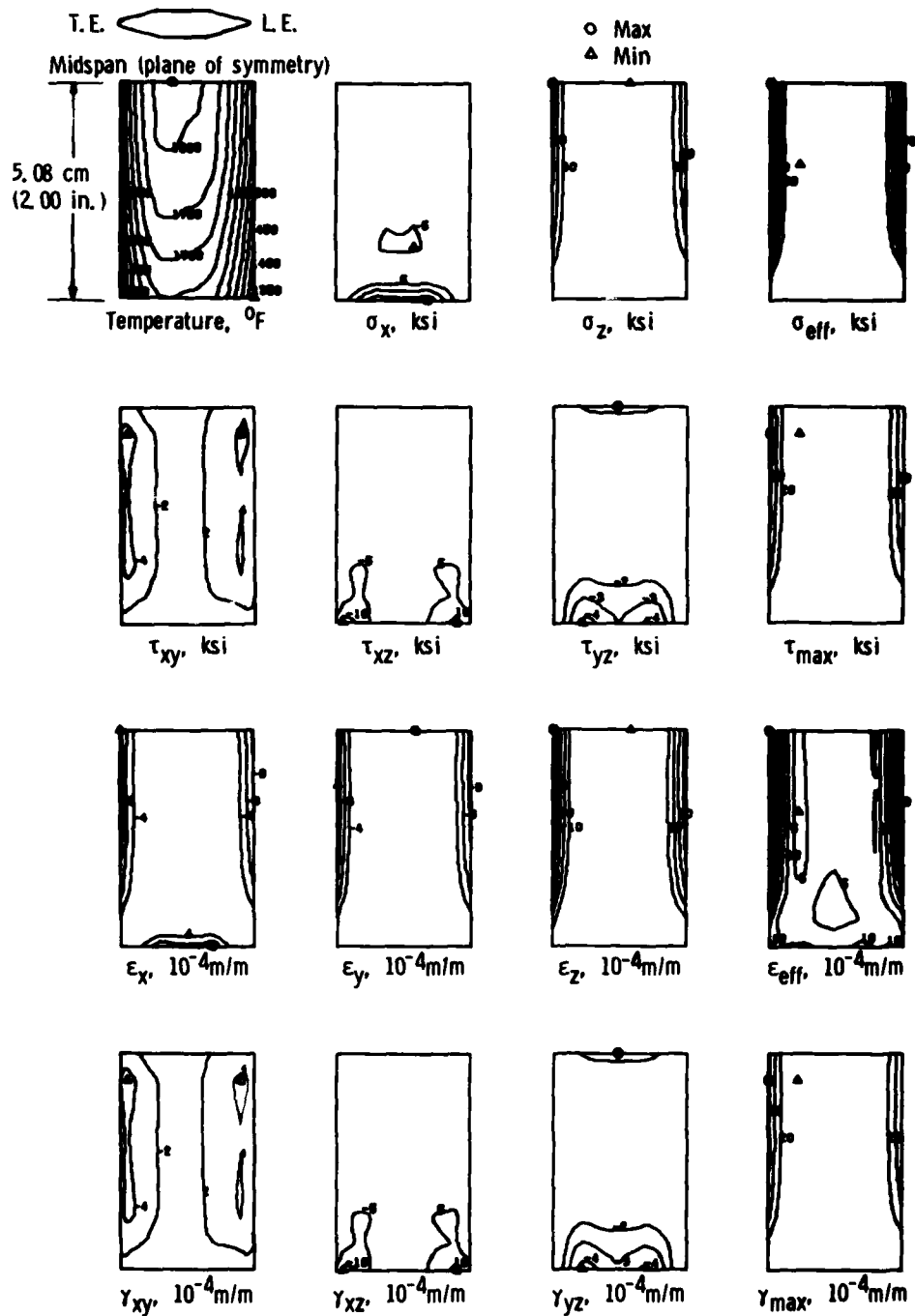
(a) IN 100 alloy after 9 seconds immersion in the cooling bed.

Figure 7. - Temperature, stress, and strain distribution of midchord at time of maximum loading edge longitudinal strain. ($F = 9/5 C + 32$)(1 ksi = 6.89×10^6 N/m²).



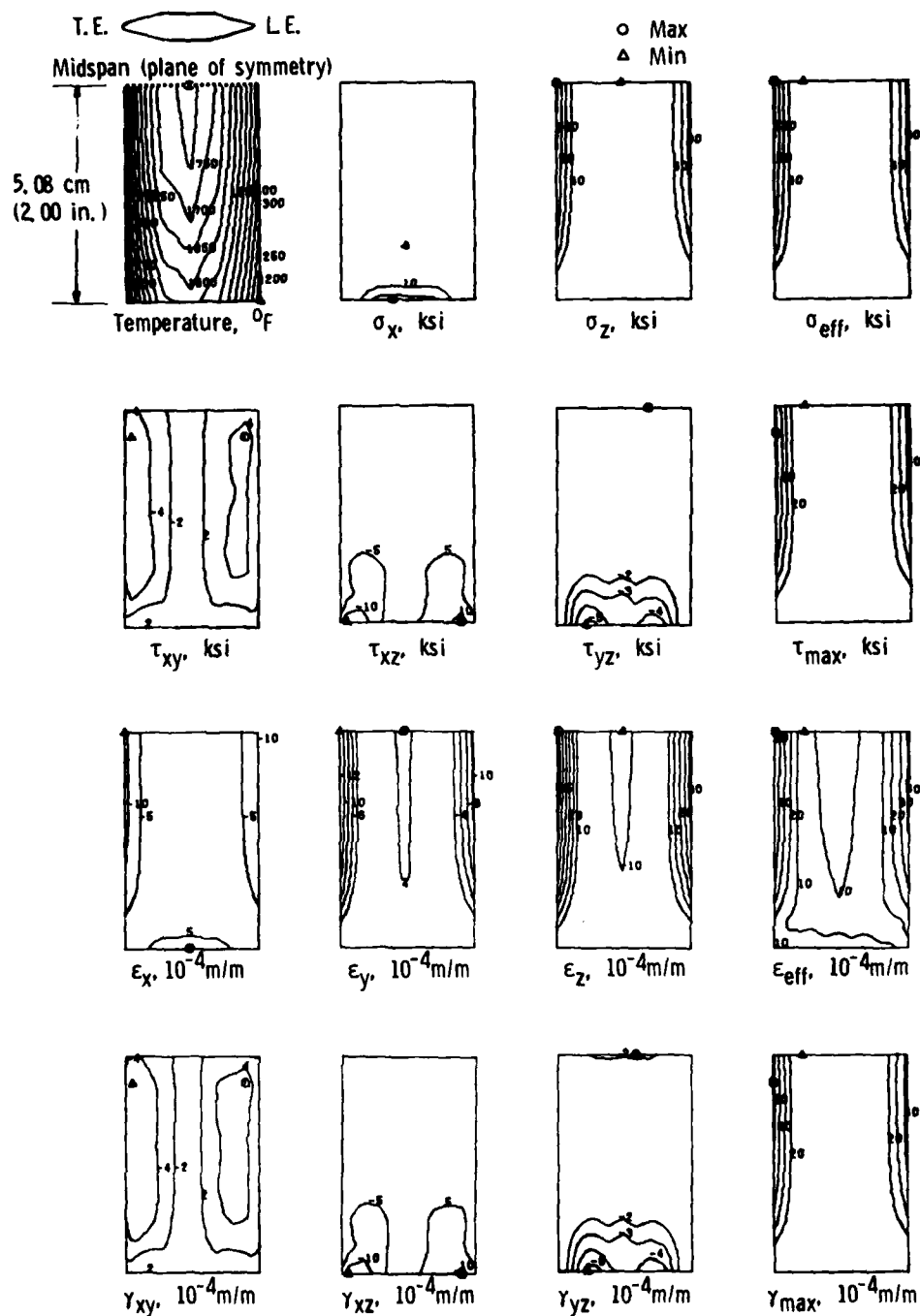
(b) Mar-M 200 alloy after 3 seconds immersion in the cooling bed.

Figure 7. - Continued.



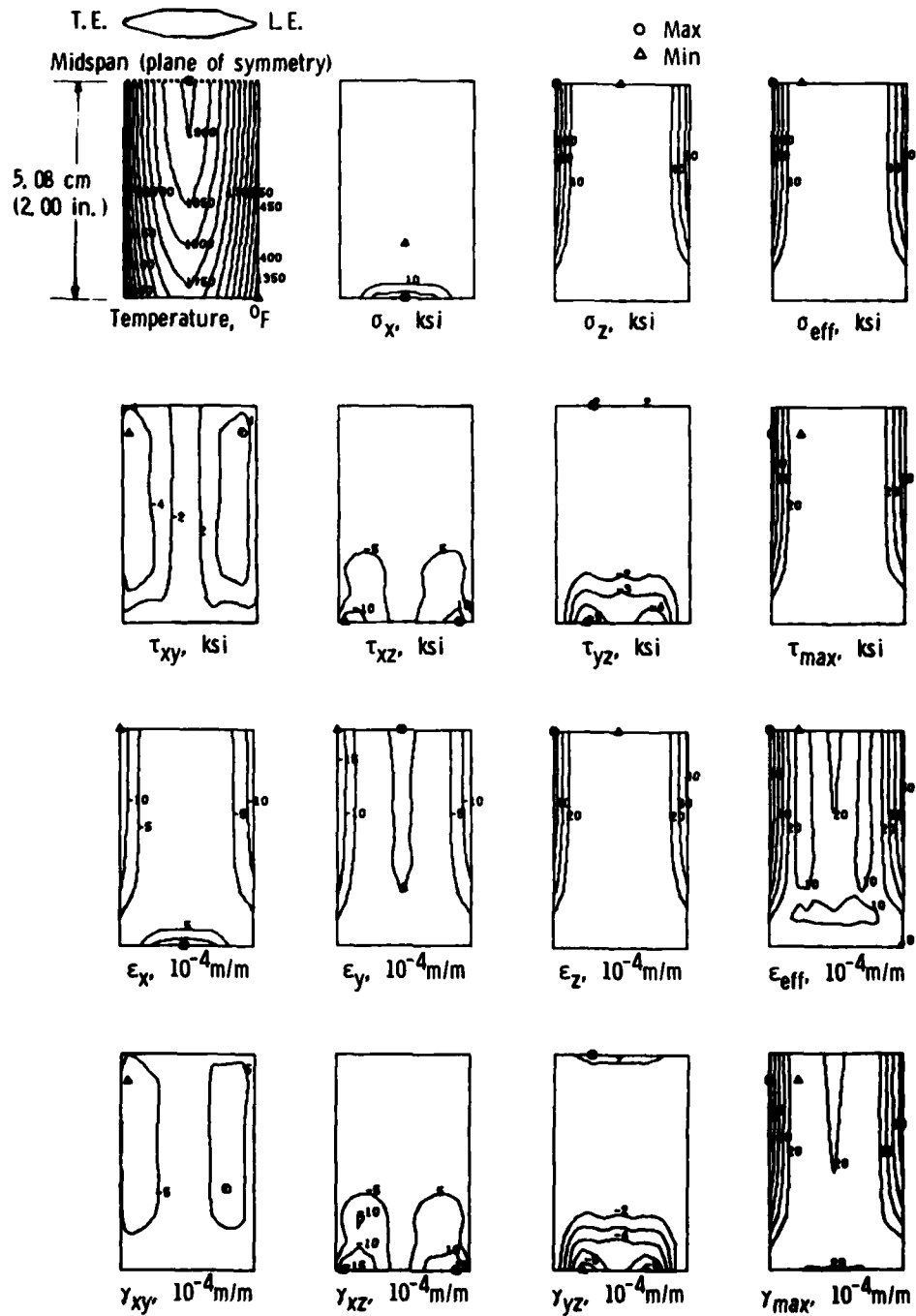
(c) Mar-M 302 alloy after 6 seconds immersion in the cooling bed.

Figure 7. - Continued.



(d) NASA TAZ-8A alloy after 15 seconds immersion in the cooling bed.

Figure 7. - Continued.



(e) Rene 80 alloy after 6 seconds immersion in the cooling bed.

Figure 7. - Concluded.

REFERENCES

1. Bizon, Peter T., and Spera, David A., Comparative Thermal Fatigue Resistance of Twenty-six Nickel- and Cobalt-Base Alloys. NASA TN D-8071, 1975.
2. Bizon, Peter T., and Oldrieve, Robert E., Thermal Fatigue Resistance of NASA TAZ-20 Alloy with Three Commercial Coatings. NASA TM X-3168, 1975.
3. Spera, David A., Howes, Maurice A. H., and Bizon, Peter T., Thermal Fatigue Resistance of 15 High-Temperature Alloys Determined by the Fluidized-Bed Technique. NASA TM X-52975, 1971.
4. Howes, Maurice A. H., Thermal Fatigue Data on 15 Nickel- and Cobalt-Base Alloys. (IITRI-B6078-38, IIT Research Institute, NASA Contract NAS3-9411). NASA CR-72738, 1970.
5. Howes, Maurice A. H. Additional Thermal Fatigue Data on Nickel- and Cobalt-Base Superalloys, Part 1. (IITRI-B6107-34-Pt-1, IIT Research Institute, NASA Contract NAS3-14311). NASA CR-121211, 1973.
6. Howes, M. A. H., Additional Thermal Fatigue Data on Nickel- and Cobalt-Base Superalloys, Part 2. (IITRI-B6107-34-Pt-2, IIT Research Institute, NASA Contract NAS3-14311). NASA CR-121212, 1973.
7. Howes, M. A. H., Thermal Fatigue and Oxidation Data on TAZ-8A, Mar-M 200, and Udimet 700 Superalloys. (IITRI-B6124-21, IIT Research Institute, NASA Contract NAS3-17787). NASA CR-134775, 1975.
8. Hill, V. L., and Humphreys, V. E., Thermal Fatigue and Oxidation Data of Superalloys Including Directionally Solidified Eutectics. (IITRI-B6124-48, IIT Research Institute, NASA Contract NAS3-17787). NASA CR-135272, 1977.
9. Hill, V. L., and Humphreys, V. E., Thermal Fatigue and Oxidation Data for Alloy/Braze Combinations. (IITRI-B-6134-25, IIT Research Institute, NASA Contract NAS3-18942), NASA CR-135299, 1977.
10. Hirschberg, M. H., and Halford, G. R., Use of Strainrange Partitioning to Predict High-Temperature Low-Cycle Fatigue Life. NASA TN D-8072, 1976.
11. Saltsman, J. F. and Halford, G. R., "Application of Strainrange Partitioning to the Prediction of Creep-Fatigue Lives of AISI Types 304 and 316 Stainless Steel." *J. Pressure Vessel Technol.*, Vol. 99, No. 2, May 1977, pp. 264-271. (NASA TM X-71898, 1976).
12. Hirschberg, M. H., and Halford, G. R., Strainrange Partitioning: A Tool for Characterizing High Temperature Low Cycle Fatigue - Materials Fatigue Test. NASA TM X-71691, 1975.

REFERENCES (CONCLUDED)

13. Halford, G. R., Saltsman, J. F., and Hirschberg, M. H., Ductility Normalized-Strainrange Partitioning Life Relations for Creep-Fatigue Life Prediction. NASA TM-73737, 1977.
14. Halford, G. R., Hirschberg, M. H., and Manson, S. S., Creep Fatigue Analysis by Strain-Range Partitioning. NASA TM X-67838, 1971.
15. Spera, David A., and Grisaffe, Salvatore, J., Life Prediction of Turbine Components: Ongoing Studies at the NASA Lewis Research. NASA TM X-2664, 1973.
16. Bizon, P. T., Hill, R. J., Williams, B. P., Drake, S. K., and Kladden, J. L., Three Dimensional Finite Element Elastic Analysis of a Thermally Cycled Single-Edge Wedge Geometry Specimen, NASA TM 79026, 1979.
17. Fritz, Louis J., and Koster, W. P., Tensile and Creep Rupture Properties of (16) Uncoated and (2) Coated Engineering Alloys at Elevated Temperatures. (Rept.-931-21300, Metcut Research Associates, Inc., NASA Contract NAS3-18911). NASA CR-135138, 1977.
18. Wolf, J., ed., Aerospace Structural Metals Handbook, Mechanical Properties Data Center, Belfour Stulen, Inc., 1978. AFML-TR-68-115, Revised.
19. Alderson, R. G., et al., Turbine Engine Components Stress Simulation Program. AiResearch-74-210816(32), AiResearch Manufacturing Co., 1977 (AFAPL-TR-77-72).
20. User's Manual - Programs MESH3, ISO3DQ, and PROUT3 Turbine Engine Components Stress Simulation Program. Rept. 74-210860(2)-1A, AiResearch Mfg. Co., Mar. 1977. (Air Force Aero Propulsion Laboratory Contract F33615-74-C-2012).
21. The NASTRAN Theoretical Manual (Level 16.0). NASA SP-221(03), 1976.
22. The NASTRAN Programmer's Manual (Level 16.0). NASA SP-223(03), 1976.
23. The NASTRAN User's Manual (Level 16.0 Supplement). NASA SP-222(03), 1976.
24. The NASTRAN Demonstration Problem Manual (Level 16.0). NASA SP-224(03), 1976.
25. Hoffman, Oscar, and Sachs, George, Introduction to the Theory of Plasticity for Engineers, McGraw-Hill Book Co., Inc., 1953, p. 28.